2013

SIRT6 and Premature Aging of Hutchinson-Gilford Progeria Syndrome Fibroblasts.

Helal Endisha
Virginia Commonwealth University

SIRT6 and Premature Aging of Hutchinson-Gilford Progeria Syndrome Fibroblasts.

A thesis submitted in partial fulfillment of the requirements for the Master of Science in Molecular Biology and Genetics at Virginia Commonwealth University.

By

Helal Abdurrazak Ali Endisha

Bachelors of Science in Pharmacy and Biotechnology from the German University in Cairo, 2011.

Director: Gail E. Christie, Ph.D

Department of Microbiology and Immunology

Virginia Commonwealth University

Richmond, Virginia

November, 2013

Acknowledgment

First and foremost I would like to thank God for giving me wisdom, strength, and guidance throughout my research work. I would like to express my deep and sincere gratitude to my research supervisor, Dr. Lynne Elmore for her help and direction with this project. I am very grateful to her for the time she spent in reviewing my thesis with great care and attention, and for her invaluable comments and suggestions that contributed much to the improvement and completion of my thesis. It was a great privilege and honor to work and study under her guidance. I would like to thank my committee members, Dr. Colleen Jackson-Cook and Dr. Joseph Landry, for their valuable input and the effort they spent in reviewing my thesis. I owe many thanks to my program director, Dr. Gail Christie who helped me tremendously during my application process and all the way through to graduating. I would also like to thank my friends and family both at VCU and globally, for their constant love, support and much needed words of encouragement. Last but not least, no words are sufficient to express my everlasting gratitude, appreciation and thanks to my beloved parents, Abdurrazak and Enaam. Without your support, prayers and faith in me, it would have been impossible for me to be where I am today. And for that, I thank you.

I would like to dedicate this research project to Sam Berns, a 17 year old young man who lives with progeria. His positive outlook on life despite the challenges he has endured and continues to endure will forever be an inspiration to me.

Table of Contents

List of Tables

List of Figures

Abstract

SIRT6 AND PREMATURE AGING OF HUTCHINSON-GILFORD PROGERIA SYNDROME FIBROBLASTS.

By Helal A. Endisha, MSc.

A thesis submitted in partial fulfillment of the requirements for the Master of Science in Molecular Biology and Genetics at Virginia Commonwealth University.

Virginia Commonwealth University, 2013.

Major Director: Gail E. Christie, Ph.D.

Department of Microbiology and Immunology

The genetic disease Hutchinson-Gilford Progeria Syndrome (HGPS) arises from a *de novo* single nucleotide mutation (1824C→T) in the *LMNA* gene. As a result, the mutated lamin A protein (progerin) remains farnesylated and permanently attached to the nuclear membrane. Progerin accumulates and deforms the nuclear membrane leading to an array of cellular abnormalities

driving the cells to enter a state of permanent cell-cycle arrest early on in replicative age i.e. premature cellular senescence. Cellular senescence has been extensively studied as one of the contributing factors to aging in HGPS patients and other age-related diseases. There has also been evidence to show that aging is accompanied by epigenetic changes and that epigenetic manipulation can incite progeroid syndromes in mice. It has been found in this study that HGPS fibroblasts express distinctly lower levels of SIRT6, a member of the sirtuin family of NAD-dependent protein deacetylases/ADP-ribosyltransferases, than normal fibroblasts. Findings from this study demonstrate that overexpression of SIRT6 prevents a decrease in replicative capacity and the onset of premature senescence in HGPS fibroblasts. Thus, SIRT6 may have promising therapeutic implications for improving HGPS age-related pathologies.

1.INTRODUCTION

1.1 Hutchinson-Gilford Progeria Syndrome: Clinical Manifestations and Challenges

Hutchinson-Gilford Progeria Syndrome (HGPS) is a rare, fatal genetic disease affecting 1 in 4-8 million people worldwide, in which the individual undergoes an advanced aging process.[1] Despite being born with a *de novo* mutation[2,3,5], affected individuals display no signs of disease at birth with symptoms manifesting at age 1 or 2 years.[1,3] Symptoms are first noticed as a 'failure to thrive' and progress into alopecia (loss of hair including scalp and eyebrows), wrinkled skin, frailty, loss of subcutaneous fat, skeletal dysplasia and hypoplasia, dry and thin skin, and osteoporosis.[1] These symptoms leave young children with the appearance and health conditions of an aged individual (Figure 1). HGPS is coined a "segmental aging syndrome" as patients lack certain typical features of aging such as neurocognitive decline or increased incidence of cancer.[4] In 90% of individuals with HGPS, death typically occurs at a mean age of 13 due to progressive atherosclerosis of the coronary and cerebrovascular arteries.[3]

1.2 HGPS: Molecular Pathogenesis

Lamins are filamentous structures present in the nuclear membrane that are essential for regulating chromatin, nuclear integrity and nuclear shape.[4] About 90% of HGPS cases (referred to as 'typical HGPS') are due to a *de novo* single nucleotide substitution in which a cytosine is mutated to a thymine at position 1824 of the *LMNA* gene which encodes for lamin A and its

exon 10 splice variant, lamin C.[2,5,30] The mutation results in a silent polymorphism (G608G), which consequently activates a cryptic splice donor site resulting in a truncated prelamin A transcript and ultimately, a mutated lamin A product with a 50 amino-acid deletion (progerin).[5] The less characterized atypical progeroid syndrome (APS) makes up the remaining 10% of HGPS cases. APS cases are the result of different heterozygous missense LMNA mutations such as P4R, E111K, D136H, E159K, and C588R. Individuals with APS display a slightly delayed onset of clinical manifestations and live for as long as a reported 51 years.[6] There has also been reported cases of the occurance of APS in siblings from parental consanguineous families, suggesting an alternative pattern of autosomal recessive inheritance.[7]

Under normal conditions, prelamin A undergoes a series of posttranslational modifications required for the production of mature lamin A protein and subsequent incorporation into the nuclear lamina (Figure 2). The prelamin A protein contains a C-terminal CAAX motif (C: cysteine; A: aliphatic amino acid; X: any amino acid) where a farensyl group (C15) is added to the cysteine by the enzyme farensyltransferase, rendering the protein more hydrophobic and allowing it to be embedded in the nuclear membrane.[8,9] The three terminal amino acids are then cleaved by the ZMPSTE24 endoprotease followed by carboxymethylation of the terminal farnesylated cysteine. A second cleavage step by ZMPSTE24 removes the modified cysteine along with 14 amino acids upstream of it allowing the mature lamin A to be released from the nuclear membrane and inserted into the nuclear lamina. The second ZMPSTE24 cleavage site of prelamin A is within the 50 amino acids missing from individuals with typical HGPS. Consequently, the mutated lamin A protein is permanently farnesylated and irreversibly

anchored in the nuclear membrane.[9] Since the alternate splice site is used about 40% of the time during prelamin A processing, the loss of lamin A and accumulation of progerin[1] disrupts normal lamina function and results in nuclear abnormalities such as laminal thickening, blebs, disrupted heterochromatin structure and clustering of nuclear pores.[10] It is conjectured that progerin-mediated aberrations cause cells to exit the cell cycle and undergo cellular senescence (see section 1.3). Furthermore, it is believed that an accumulation of senescent cells disrupts tissue homeostasis and contributes to organismal aging.[11] In the case of HGPS, induction of cellular senescence occurs at a much more rapid pace, presumably contributing to the pathological aging phenotypes so characteristic of this progeroid syndrome.

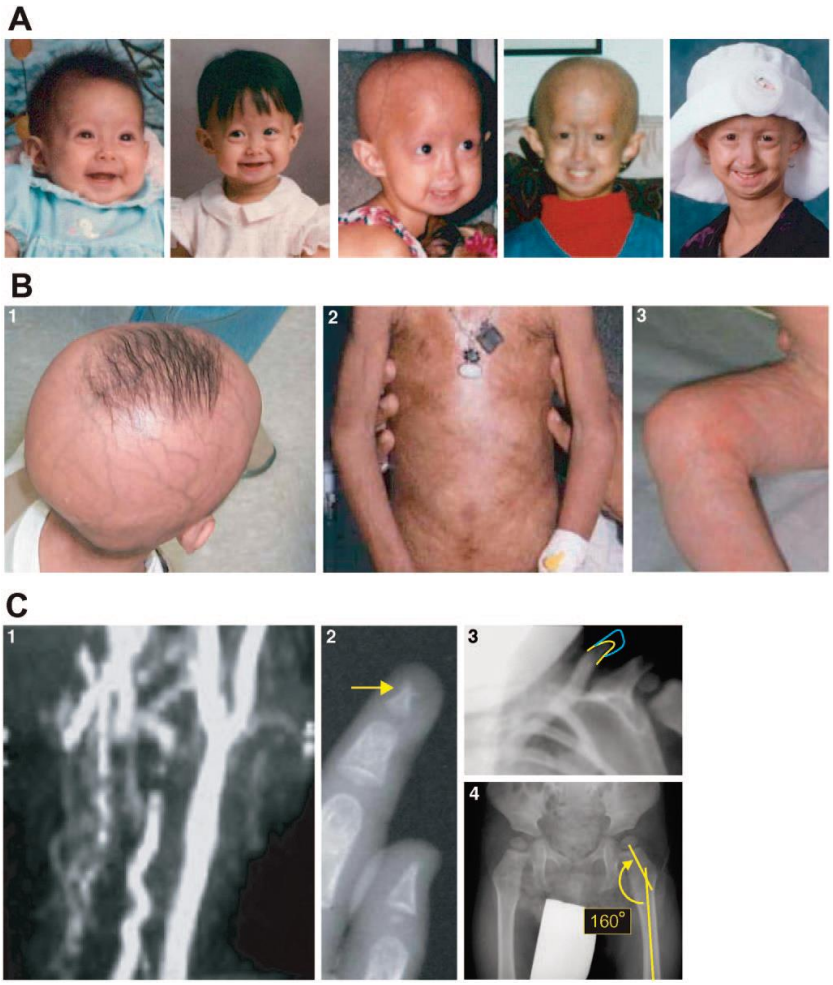

Figure 1. Physical Characteristics of HGPS with Age. *(A)* A girl with HGPS at ages 3 months, 13 months, 3 years 11 months, 6 years 6 months, and 9 years. *(B1)* Representative image of alopecia in a 3-year old child with progeria. *(B2)* Representative image showing skin findings in a 7-year old child with progeria. The image shows areas of discoloration, speckled pigmentation, and tight skin restricting movement. *(B3)* Knee joint restriction in a 3-year old child with progeria. *(C1)* Carotid artery MRI in a 4-year old with progeria demonstrating patency of the right common carotid artery and complete occlusion of the left common carotid artery. *(C2)* Radiographic image indicating acroosteolysis (i.e. resorption of the distal bony phalanges) with an ill-defined phalangeal edge. *(C3)* Clavicular resorption. *(C4)* Coxa valga i.e. deformity of the hip where the angle formed between the head and neck of the femur and its shaft is increased. (Photos and MRIs are courtesy of the Progeria Research Foundation)

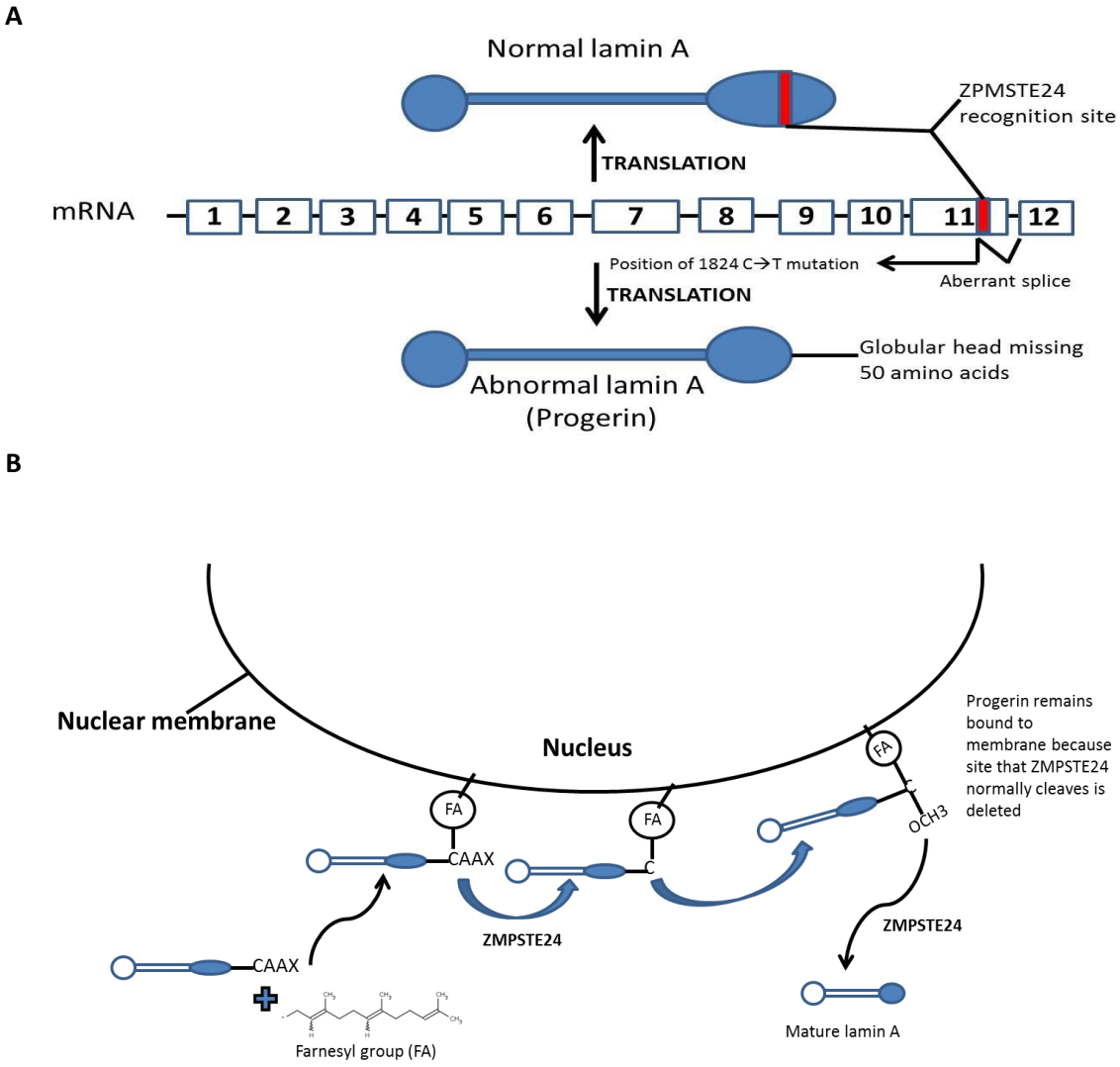

Figure 2. Effects of the *LMNA* Mutation on Posttranslational Modifications in HGPS. *(A)* Normal splicing results in lamin A. The 1824 C→T mutation in typical HGPS activates a cryptic splice donor site in exon 11 that deletes 150 bases from the mRNA. The resulting truncated abnormal lamin A protein is called progerin. *(B)* Posttranslational lamin A processing. A farnesyl group binds to the cysteine residue (C) at the C-terminal by the enzyme farnesyltransferase. The lamin A binds to the membrane of the endoplasmic reticulum by means of the farnesyl group. ZMPSTE24 then cleaves the terminal three amino acids, after which the farnesylated cysteine is carboxymethylated ($0CH_3$). ZMPSTE24 then cleaves the modified cysteine along with 14 amino acids upstream of it releasing the mature lamin A. Due to the abnormal splice, the ZMPSTE24 recognition site is deleted in HGPS and progerin remains farnesylated and bound to the membrane.

Figure adapted from "Hutchinson-Gilford progeria syndrome, aging, and the nuclear lamina." Korf B. (2008), 358(6), 552-555.

1.3 Telomeres and Senescence

A recent review ("The Hallmarks of Aging") characterized aging as 'the time-dependent functional decline that affects most living organisms'.[11] They propose as many as 9 possible hallmarks that contribute to organismal aging. Genetic instability (discussed later) and telomere attrition due to defects in nuclear architecture are two of the suggested hallmarks. Normal cells have a finite replicative potential depending in part on their species and tissue origins, age of donor and genetic background, eventually undergoing senescence.[12] Telomeres are DNA sequences at the end of chromosomes that are characterized by tandem repeats of TTAGGG in vertebrates. The length of repeats at chromosome ends varies between individual chromosomes and also varies depending on tissue type, donor age (chronological age) and the replicative history (physiological age) of the cells.[13] However, a minimum number of repeats are required at chromosome ends to recruit sufficient telomere-specific proteins for the formation of functional telomeres that differentiates normal ends from double-stranded breaks. Telomeres can be extended by a ribonucleoprotein complex called telomerase, which is composed of a protein component (Telomerase Reverse Transcriptase (TERT)) and an RNA primer sequence (Telomerase RNA Component (TERC)).[14] Some cancers achieve telomere elongation via the Alternative Lengthening of Telomeres (ALT) pathway, which relies on recombination-mediated elongation.[15] Telomeres play a role in ensuring chromosomal stability by preventing end-to-end fusions of chromosomes and proper segregation of genetic material into daughter cells during cell division.[13] In most mammalian somatic cells, telomeres shorten with each cell division as a result of incomplete DNA replication since telomeric DNA is replicated from internal origins and not from the very end of the chromosomes. DNA

polymerase can only synthesize DNA in a 5' to 3' direction by adding polynucleotides to RNA primers upstream along the length of the DNA. This is followed by replacement of the RNA strand with DNA. At the chromosome ends, DNA polymerase cannot replace the RNA primer because a template no longer exists in the 5' direction to place another primer.[16] This 'end replication problem' along with the lack of expression of telomerase by most normal somatic cells leads to telomere shortening with each cell cycle. Consequently, telomeres of fibroblasts from individuals of old age are much shorter than those of younger individuals.[12.13] There are numerous assays to estimate telomere length, such as by means of the length distribution of terminal restriction fragments (TRF), which contains the telomeric TTAGGG tract as well as telomere-like and non-telomeric sequences.[13,17] Germ cells, which express telomerase, have mean telomere lengths of 10-15 kb while presenescent cultures from fetal or neonatal tissues typically have mean telomere lengths of 8-10 kb.[18] Somatic cells lose 50-200 bp per doubling.[19] Telomere loss can also occur due to sporadic events such as failed telomeric DNA repair or problems during replication. The progressive attrition of telomeric DNA leads to a loss of the telomere capping proteins, exposing DNA breaks that activate cell cycle arrest and senescence (telomere-dependent senescence).[20] The resulting limitation in the replicative potential of cells that have undergone telomere shortening with age limits their proliferation and leads to the loss of cells and tissue function. Unlike germ cells, stem cells and cancer cells, somatic cells lack telomerase activity and gradual telomere loss and senescence are inevitable.[21] Ectopic expression of hTERT has been demonstrated in many studies[22,23] to extend cellular lifespan (normal human diploid fibroblasts and HGPS fibroblasts) to at least twice the life span at which

the uninfected cultures senesced (30-60 population doublings for normal fibroblasts), thus extending *in vitro* lifespan.[24]

Previous research[12] has shown that when compared with age-matched controls, the average telomere length in fibroblasts from HGPS patients was significantly shorter.[25] The abnormally short telomere length in HGPS fibroblasts was not seen in HGPS hematopoietic cells which either did not express detectable LMNA or expressed it at much lower levels.[12] This suggests that the expression of progerin (either direct or indirect) is involved in the generation of short telomeres. Since telomeres have been shown to attach to the nuclear matrix, dysfunction of the nuclear architecture in HGPS may impair telomere structure and function. The lamina serves as a scaffold for multi-protein and chromatin containing complexes, which have a role in the maintenance, repair and replication of telomeric DNA, the disruption of which could lead to an increase in replication errors, failure to repair DNA damage and impairment in the accessibility of enzymes.[14] Thus, the lamina has been suggested to have a critical role in the maintenance of telomere length.[12]

During cellular senescence, normal fibroblasts change their morphology from a spindle shape to an enlarged, flattened and irregular shape. Using senescence-associated β-Galactosidase (SA β-gal) as a histochemical biomarker, senescent cells can be identified by the expression of a lysosomal β-galactosidase enzyme, which cleaves the substrate X-Gal at pH 6 forming a blue precipitate.[26] During exponential growth, replicative age in culture can measured in terms of population doublings (PDs).

Thus, pathological telomere dysfunction in HGPS has been reported to be caused by aspects such as dysfunctional nuclear architecture due to progerin accumulation, rapid telomere shortening, and an inherently shorter than average telomere length.[12] It is believed that the resulting premature cellular senescence is one of the major elements contributing to the accelerated aging phenotypes developing in children with HGPS.[11]

Apart from telomere dysfunction, cellular senescence can be triggered by a multitude of factors including, but not limited to, stress, oncogene activation, chromatin perturbation (discussed later), and DNA damage.[52]

1.4 DNA Damage and Cellular Senescence

It has been revealed that low levels of progerin protein are present in skin derived from elderly individuals. In normal fibroblast cultures, progerin expression appeared to accumulate with increasing replicative age, albeit still relatively low when compared to the amount of progerin accumulating in HGPS fibroblastic cultures.[3,10,30] Research by McClintock et al.[30] suggests that progerin expression may be a biomarker of normal cellular aging and a precursor for senescence in older individuals. In addition to their structural functions, lamins form nucleoplasmic foci containing the replicative proteins PCNA (proliferating-cell nuclear antigen) and DNA polymerase δ, both of which are necessary for the systematic initiation of S-phase replication in particular, fork progression at replication centers. The accumulation of progerin on the nuclear membrane results in a loss of these nucleoplasmic lamin A foci, causing

replication fork stalling and DNA double-strand breaks (DSBs) as well as a loss of heterochromatin and dysmorphic interphase nuclei.[31]

Another consequence of progerin accumulation and lamina disruption is the failure to repair DNA damage, as previously mentioned (see section 1.3). DNA damage accumulation, the reduction of replicative proteins and the prevention of access of DNA repair proteins to sites of DNA DSB (discussed later), are collectively responsible for the phenotypes associated with HGPS and may have causal roles in normal aging.[21] The accumulation of DNA damage activates DNA damage and replication checkpoints, which reduce cell cycle progression and halts replication, thus preventing DNA lesions from being converted to inheritable mutations.[32] The two main kinases responsible for initiating these checkpoints are Ataxia-Telangiectasia Mutated (ATM) and ATM- and Rad3-Related Protein (ATR). There are two main checkpoints during the cell cycle controlling cell division, the G1/S and the G2/M, whose functions are to assess DNA damage detected by sensor mechanisms. ATM plays a role in cell-cycle delay in response to DNA DSBs, while ATR is activated by a broad range of DNA damage and replication interference.[32,33] D'Adda di Fagagna et al.[32] reported that in telomere-initiated senescence, a checkpoint response similar to that in cells with DNA damage stress was activated involving ATM, ATR and their downstream kinases Checkpoint Kinase 1 (CHK1) and Checkpoint Kinase 2 (CHK2). The activation of ATM and ATR is identified by their clustering into distinct nuclear foci and it is their activation that is responsible for decreased cell cycling and reduced replicative capacity in aged progeroid cells.[32] This led researchers to assume that DNA damage response

and telomere-initiated senescence activate the same signaling pathway. However, to determine whether the activation of ATM and ATR is directly related to the accumulation of progerin, Liu et al.[33,34] transfected HeLa (cervical cancer) cells with progerin. By immunofluorescence analysis, they observed translocation of the checkpoint kinases to the nucleus, in contrast to cells transfected with an empty vector which showed most of ATR located in the cytoplasm. This finding indicated that the accumulation of progerin led to the activation of ATM and ATR due to accumulated DNA damage, which contributes to both aging and cellular senescence.[21]

A family of proteins required for the phosphorylation and activation of the ATM and ATR checkpoint kinases are the BRCA1 C Terminus (BRCT) domain. 53BP1 (p53-binding protein 1), a member of the BRCT protein family, is one of the mediators between early detection of a DNA lesion and the transducer kinases such as CHK1 and CHK2, which target downstream DNA-damage response components, including p53.[35,36] Phosphorylation of the transcriptional regulator, p53, by ATM and kinases downstream of ATM results in cell cycle arrest (senescence) or apoptosis to prevent DNA replication and cell division in the presence of DNA damage.[21] 53BP1 undergoes nuclear relocalization to focal structures in response to DNA damage to aid in DNA repair. Knockout of *53Bp1* (*53Bp1*$^{-/-}$) leads to genome instability characterized by increased levels of chromatid gaps, breaks and exchanges in addition to aneuploidy and tetraploidy in the absence of exogenous DNA damage. Furthermore, *53Bp1*$^{-/-}$ cell lines exhibit elevated sensitivity to exogenous DNA damage relative to wild-type cells, verifying the involvement of 53BP1 in DNA repair.[36] Using 53BP1 foci as an indicator of DNA DSBs, Liu et al.[38] observed significantly more 53BP1-positive DNA damage foci per nuclei in primary dermal fibroblasts from 2 different

HGPS strains than those observed in normal fibroblast controls, indicating greater DNA DSBs in these progeria cells.

Low passage HGPS cells grow relatively well when compared to normal human primary fibroblasts; however their growth capacity is limited and they quickly begin to senesce.[14] An increase in dysmorphic nuclei and number of γH2AX (phosphorylated histone H2AX) foci are seen. H2AX is a minor histone H2A variant, which is phosphorylated at Ser^{139} to γH2AX and is important for sensing early detection of a DSB. γH2AX is required for the focal recruitment of 53BP1 and other DNA repair factors.[32] Similar to 53BP1 foci; it is used as a surrogate for nuclear sites of DSBs. As HGPS cells are passaged in culture, they accumulate endogenous DNA damage and exhibit higher levels of γH2AX. Increased levels of phosphorylated CHK1 and CHK2 are also seen as a result of persistent ATM and ATR activation, which ultimately results in cell growth arrest in HGPS cells.[31]

Zou et al.[31], have reported that the accumulation of DSBs in HGPS is likely due to a deficiency in DNA repair. They found that in HGPS cells, xeroderma pigmentosum group A (XPA), which is normally an essential factor for nucleotide excision repair (NER), binds to the stalled replication forks, denying the access of repair proteins such as Rad50, Rad51 and 53BP1 to the DSBs for repair. As a result, the accumulation of DSBs is implicated in the genome instability presented.

Collectively, findings in the literature indicate that DNA damage is accumulated in HGPS cells as a result of defective DSB repair. The DNA repair failure is not a result of defects in the DNA repair machinery; rather, it is more likely due to the dysfunctional nuclear architecture in HGPS cells. The persistent activation of the ATM/ATR pathway and subsequent cell cycle arrest drive

the cells to enter a senescent state. Moreover, the restricted access of repair proteins to sites of DSBs due to bound XPA leads to an accumulation of unrepaired DSBs. Whereas DNA repair or damage response genes are not defective in this laminopathy, a connection exists between the mutated lamin A proteins and the disruption of DNA metabolism resulting in genome instability and premature aging phenotypes.[29]

1.5 Current Therapeutic Treatments

A class of drugs called farnesyl transferase inhibitors (FTIs) used to treat progeria cells *in vitro* demonstrated amelioration of the morphologic nuclear abnormalities such as laminal thickening and blebbling.[4] In a clinical trial published in 2012,[27] weight gain, improved bone structure and increased flexibility of blood vessels were observed in children. FTIs act by reversibly binding to the farensyltransferase CAAX binding site, thus inhibiting progerin farensylation and its incorporation into the nuclear membrane.[27] FTIs exhibit partial correction of the abnormal cellular and disease phenotypes, and delay mortality in progerin-expressing mice; however, the levels of γH2AX and phosphorylated CHK1 and CHK2 in HGPS cells were not reduced, neither was the frequency of DSBs suggesting that the restoration of nuclear shape is not sufficient to overcome the genomic instability present in HGPS cells.[3,28,33]

Thus, progerin farnesylation is found to contribute to the toxicity arising from the accumulation of progerin, however, there must be other factors accounting for the genomic instability seen in HGPS fibroblasts. Whereas DNA repair or damage response genes are not defective in this laminopathy, a connection exists between the mutated lamin A proteins and the disruption of DNA metabolism resulting in genome instability and premature aging phenotypes.[29]

1.6 The Role of Sirtuins in DNA Repair and Aging

As previously mentioned, both genomic instability and telomere attrition contribute to cellular senescence, which itself contributes to aging. Additionally, alterations in DNA methylation patterns, histone modifications, and chromatin remodeling all constitute age-associated epigenetic changes.[11] Members of the sirtuin family of NAD^+-dependent protein deacetylases and ADP ribosyltransferases have been widely studied as potential anti-aging factors.[39-44] The Silent Information Regulator-2 gene (Sir2) encodes an NAD-dependent histone deacetylase that links chromatin regulation, genomic stability, and life span in Saccharomyces cerevisiae, a species of yeast. By means of chromatin silencing, Sir2 inhibits transcription and suppresses recombination at ribosomal DNA (rDNA) repeats.[39,40,42] In S. cerevisiae with mutations in Sir2, increased genomic instability indicated by recombination at ribosomal DNA (rDNA) repeats is seen. This ultimately leads to a shortened replicative life span. Homologous recombination between rDNA repeats leads to the formation of rDNA circles, which causes senescence in yeast and is thought to be the process by which yeast age.[46] An overexpression of sir2 was found to prevent the accumulation of rDNA circles and thus increase replicative life span.[46] The increase in lifespan due to extra copies of sir2 was reported not only in yeast, but also in the multicellular organisms, C. elegans and D. melanogaster.[41]

There are seven Sir2 family members in mammals; SIRT1-SIRT7.[39] Of particular interest in the context of regulation of life span, chromatin and genomic integrity is the mammalian SIRT6. Mostoslavsky et al.[42] found the SIRT6 protein to be primarily nuclear by immunostaining and

co-fractioned with histones within the chromatin/nuclear matrix subfraction, indicating that the SIRT6 protein favorably associates with chromatin within the nucleus. Furthermore, SIRT6$^{-/-}$ mice were generated and showed no abnormalities at birth apart from a reduced body size shortly after birth. At about 3 weeks, the mice exhibited degenerative phenotypes such as loss of subcutaneous fat, lordokyphosis, colitis, severe lymphopenia and failed to thrive. The mice ultimately died at postnatal day 24. Recalling the phenotypes expressed in children with HGPS, SIRT6$^{-/-}$ mice exhibited some overlapping pathologies with those of premature aging. These findings hint that there may be a role for SIRT6 in the regulation of life span and perhaps the prevention of the development of progeroid pathologies.

SIRT6 has been found to deacetylate the histone H3 lysine 9 residue (H3K9) at the telomeres consequently stabilizing the association of the Werner protein (WRN) with telomeres.[44] WRN is a DNA metabolic factor, which helps maintain the structure and integrity of DNA and is mutated in another form of progeria, Werner Syndrome.[40] The depletion of SIRT6 in human diploid fibroblasts by SIRT6 knockdown significantly inhibited the association of WRN with telomeric chromatin.[44] The subsequent telomere dysfunction and genomic instability implied a requirement of SIRT6 for the stabilization of WRN with telomeric chromatin. In addition, SIRT6 is recruited and deacetylates H3K9 at the promoters of genes activated by the NF-κB transcription factor, silencing gene expression and limiting NF-κB signaling.[39] Hyperactive NF-κB signaling is a significant factor resulting in degenerative phenotypes and early death in SIRT6-deficient mice, revealing a potential role for SIRT6 in the regulation of gene expression and its effect on genomic stability and aging.[40]

McCord et al.[40] have shown that SIRT6 plays a role in DNA DSB repair. They report that SIRT6 associates with chromatin in response to DNA damage and stabilizes the DNA DSB repair factor, DNA-dependent kinase (DNA-PK), at the DSBs. The DNA-PK holoenzyme is a central regulator of DNA DSB repair in mammalian cells.[40] Through the use of a stringent chromatin fractionation protocol, McCord et al.[40] revealed that upon DNA damage, more SIRT6 associates with chromatin, indicating a possible dynamic association of SIRT6 with chromatin modulated by DNA damage. Furthermore, upon the generation of DNA DSBs, increased levels of chromatin-associated DNA-PKs were observed when compared to no change in DNA-PKs levels in SIRT6 knock down (KD) cells. To determine whether increasing SIRT6 levels can further drive DNA-PKs to DSBs, SIRT6 was overexpressed using a retrovirus in HeLa cells. About a 3 fold increase in DNA-PKs was observed at the DSB, in contrast to a reduction in the DNA-PKs signal in cells expressing the catalytically inactive SIRT6 mutant protein.[40] Collectively, these experimental data are consistent with SIRT6 being required for the recruitment of DNA-PKs to chromosomal DSBs, highlighting the significance of SIRT6 in chromatin regulation, DNA repair and the prevention of aging-like degenerative phenotypes.

On the other end of the spectrum, in 2012, Kanfi et al.[41] showed that SIRT6 overexpression led to increased longevity in male mice further emphasizing the importance of SIRT6 in regulating mammalian longevity.

1.7 SIRT6 and its potential role in DNA repair in HGPS

SIRT6 has been associated with DNA repair and telomere maintenance, as well as having functions in attenuation of inflammation and glucose homeostasis.[49] Michishita et al.[49] reported

that *SIRT6* knockdown (S6KD) human fibroblasts have a marked shortened replicative lifespan, undergoing premature senescence (as measured by senescence-associated β-galactosidase histochemical staining) about ten population doublings before control cells. Mostoslavsky et al.[42] found that multiple independent *Sirt6*$^{-/-}$ mouse embryonic fibroblast (MEF) lines had a smaller fraction of S phase cells than control wild type cultures, indicating that the absence of Sirt6 reduces proliferative rates. These findings have lead researchers to conclude that SIRT6 is essential in maintaining a normal replicative life-span and in preventing the premature senescence *in vitro*. Furthermore, A. Cardus et al.[44] showed that in SIRT6-depleted human endothelial cells, there was a significant increase in γH2AX foci formed at sites of DNA damage and dysfunctional telomeres. They observed a concurrent increase in the appearance of telomere dysfunction-induced foci (TIFs), i.e. sites where γH2AX foci co-localized with telomere repeat binding factor-1 (TRF-1) signals suggesting that SIRT6 mitigates DNA damage and telomere dysfunction and that SIRT6 may be required for functional DNA repair.

Thus, the presence of SIRT6 has been demonstrated to protect different cell types from telomere and genomic DNA damage and improve replicative capacity. By targeting multiple cellular defects that contribute to cellular senescence, the manipulation of SIRT6 may be applied to the prevention of the onset of premature cellular senescence and improving age-related pathologies.

1.8 HYPOTHESIS

The parallels between the degenerative phenotypes observed in SIRT6-deficient cells/mice and HGPS fibroblasts/patients are striking. It is of interest to note that progeria research has led to the discovery that progerin accumulates in cultures of normal fibroblasts with increasing chronological and physiological age.[30] Histone modifications are a category of epigenetic alterations thought to contribute to cellular senescence. To date, endogenous SIRT6 expression levels have not been assessed HGPS fibroblasts. Moreover, essentially nothing is known about the effect of histone modifications via ectopic SIRT6 expression on the induction of senescence in HGPS cells. Based on experimental data generated from the aforementioned experiments, it was hypothesized that **(1) HGPS fibroblasts will express lower levels of SIRT6 protein than normal fibroblasts, which contribute to DNA damage and premature senescence, and (2) Overexpressing SIRT6 will prevent premature senescence in HGPS fibroblasts.** To test these hypotheses the following specific aims were proposed:

Aim 1: Determine the endogenous levels of SIRT6, frequency of DNA damage foci, β-galactosidase positivity and population doubling time of dermal fibroblasts derived from individuals with HGPS compared to fibroblasts from normal donors.

Aim 2: Determine whether SIRT6 overexpression in HGPS fibroblasts reduces the frequency of DNA damage foci, β-galactosidase positive staining and improves proliferative capacity.

The data generated from the proposed studies will provide novel insight into the link between epigenetic alterations and age-related pathologies in HGPS and normal fibroblasts. The ectopic expression of SIRT6 in preventing the onset of premature senescence in HGPS may offer an

innovative method to reduce the accumulated DNA damage expressed in HGPS, which was not reduced by FTIs.[33]

2. Materials and Methods

2.1 Cell Culture Methods

Table1. List of Cell Lines

Cell Line (Catalog ID)	Description	Cell Type	Sex	Age
AG01972	**HGPS**	**Fibroblast**	**Female**	**14YR**
AG11513	**HGPS**	**Fibroblast**	**Female**	**8YR**
GM00969	**Apparently healthy non-fetal tissue**	**Fibroblast**	**Female**	**2YR**
AG09602	**Gerontology Research Center Cell Culture Collection**	**Fibroblast**	**Female**	**92YR**

Source: Coriell Institute for Medical Research (Camden, NJ).

Mycoplasma (bacterial) contamination induces cellular changes such as changes in metabolism and cell growth.[47] It also poses biosafety concerns in the lab and allows for the possibility of cross-contamination. For these reasons, mycoplasma testing using the LookOut® Mycoplasma PCR Detection Kit (Sigma, MP0035) was performed on all cell cultures to ensure the validity of subsequent study results. Mycoplasma negative cells were grown at 37°C in 5%CO_2 in Minimum Essential Medium Eagle (EMEM, 1X) with Earle's salts (Cellgro) supplemented with 15% (v/v) fetal bovine serum (FBS) (Invitrogen), 100x MEM non-essential amino acids (NEAA) (Cellgro),

200mM L-Glutamine (Gibco) and antibiotic/antimycotic (ABAM) (Invitrogen). Cells were passaged by standard Trypsin-EDTA dispersion aseptically under a laminar flow hood. For long-term storage, cells were cryopreserved in cosmic calf serum (CCS) (Invitrogen) + 10% dimethyl sulfoxide (DMSO) (Fisher Scientific, BP231-100) and placed in an isopropanol freezing chamber at -80°C. Cells were then transferred to a liquid nitrogen tank.

Population doublings were calculated from cell counts taken at each passage, where PD = [log(N /Xo)] / log 2 (N=final cell count, Xo=initial cell count).

2.2 Lentiviral Infections and Constructs

SIRT6 and empty vector lentiviral supernatants were obtained from the Biological Macromolecule Shared Resource Core at Virginia Commonwealth University. The SIRT6 gene was cloned in a pcDNA3.1+ vector backbone (Addgene, Plasmid 13817) (Figure 3). SIRT6 was expressed in the pCDH-CMV-MCS-EF1-Puro expression lentivector (System Biosciences) (Figure 4), which allows for stable, efficient, long-term expression of the SIRT6 gene in the normal and HGPS fibroblasts. GM00969, AG11513 and AG01972 cells were each seeded in triplicate in 60mm dishes at a density of $2x10^5$ cells per dish. For each cell strain, a plate of uninfected cells was included as a control. Cells were infected at a multiplicity of infection of 1.0. To determine the volume of lentivirus particles to add to each well, the following equations were used:

$$Total\ number\ of\ cells/well \times desired\ MOI\ = Total\ TU\ needed$$

$$\frac{Total\ TU\ needed}{TU/ml} = Total\ ml\ of\ lentiviral\ particles\ to\ add\ to\ each\ well$$

A transduction unit per ml (TU/ml) is the measurement of how much virus infects a target cell. The estimated transduction units for the SIRT6 and empty vector lentiviral supernatants were $2x10^7$ and $1x10^7$ TU, respectively.

Media containing 10µl of SIRT6 lentiviral supernatant or 20µl of empty vector control was added to dishes that were 60-70% confluent. To increase the transduction efficiency, polybrene (Santa Cruz Biotechnology, sc-134220) was added to the media at a final concentration of 8µg/ml in all dishes including the uninfected cells. Cells were infected overnight in the incubator and replaced with fresh media the next day. After allowing the cells to recover for a day, puromycin (Sigma, P9620) was added to the culture medium to selectively kill all uninfected cells. Prior to the drug selection of infected cells, a puromycin 'Kill Curve' was performed on uninfected GM00969, AG11513 and AG01972 cells to determine the optimal concentrations of drug. Specifically, the cells were seeded at ~50% confluency into the wells of a 48-well plate with 250µl fresh medium. The next day puromycin (range 0-900ng/ml) was added to the wells. The cells were microscopically monitored every day for 5 days and the minimum concentration of puromycin that caused complete cell death in 3-5 days was selected. A puromycin concentration of 0.7µg/ml killed both normal fibroblasts and HGPS cells in 4 days.

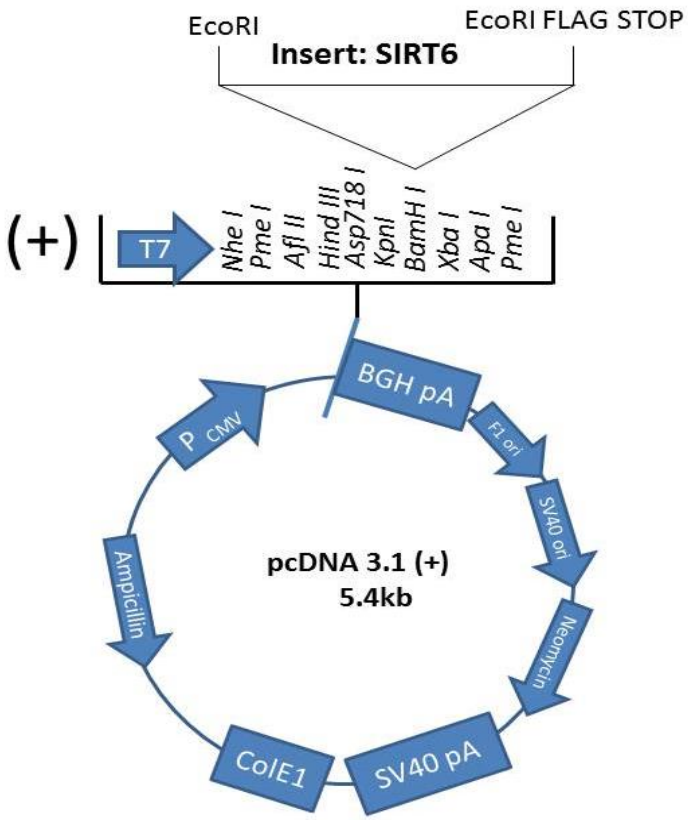

FIGURE 3. SIRT6 Gene Cloned in a pcDNA3.1+ Vector Backbone. SIRT6 was digested using EcoRI restriction enzymes from the pcDNA3.1 vector at EcoRI recognition sites.

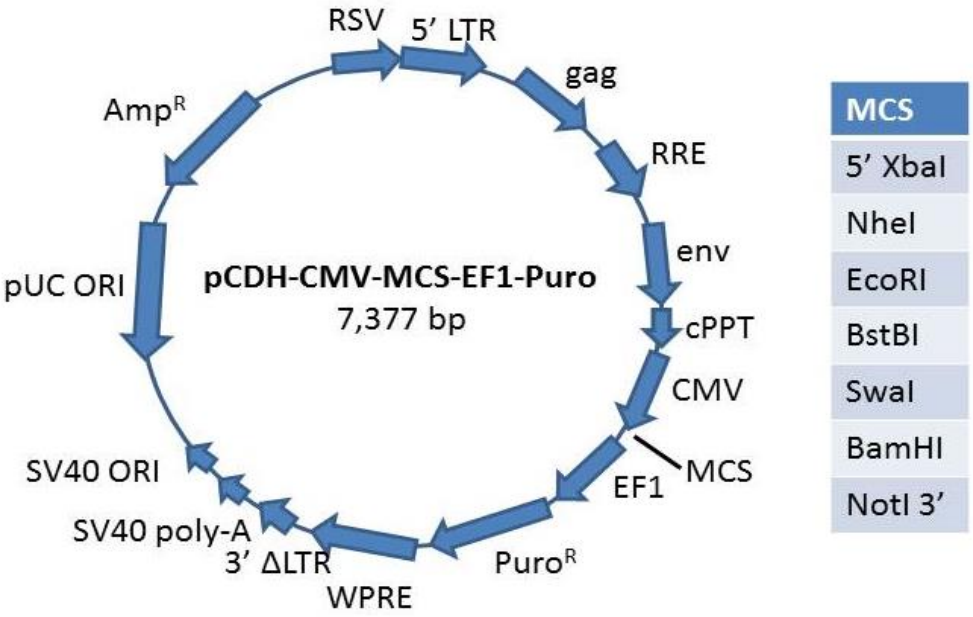

Figure 4. pCDH-CMV-MCS-EF1-Puro Lentiviral Expression Vector with a CMV Target Gene Promoter. The lentiviral vector was digested at the MCS using the same restriction enzyme (EcoRI) used to digest the pcDNA3.1 plasmid.

Key features: MCS – multiple cloning site for cloning the gene of interest; CMV – target gene promoter; SV40 polyadenylation – enables efficient termination of transcription of recombinant transcripts; SV40 origin – for stable propagation of the pCDH in mammalian cells; pUC origin – for high copy replication and maintenance of the plasmid in *E.coli* cells; Ampicillin resistance gene – for selection in *E.coli* cells; Puromycin resistance gene – Puromycin-resistant marker for selection of the transfected cells.

Human dermal fibroblasts (HDF) under Tet-on control to induce EGFP-Progerin and EGFP-Lamin A were kindly provided by Dr. Tom Misteli from the National Cancer Institute (Bethesda, MD). The fibroblasts are hTERT immortalized; therefore, population doublings were not monitored. For my experiments, fibroblasts were seeded in our standard fibroblastic growth media (EMEM + 15%FBS + 100X NEAA + 100X L-glut + 100X ABAM) supplemented with doxycycline to induce

expression of progerin. Progerin production was induced with 750ng/ml doxycycline for 4, 8 and 14 days in culture. Through correspondence with Dr. Nard Kubben from the Misteli Lab, a level of progerin equal to half the intensity of endogenous lamin A, on a western blot, was recommended to induce proper aging effects.

2.3 Antibodies

Table 2. List of the primary and secondary antibodies used.

A

PRIMARY ANTIBODIES
Rabbit anti-SIRT6 (Cell Signaling, 2590)
Mouse monoclonal anti-acetyl-Histone H3 (Ac-Lys^{9}) (Sigma, H0913)
Mouse anti-human 53BP1 (BD Transduction Laboratories, 612523)
Mouse anti-progerin antibody (Abcam, ab66587)
Mouse monoclonal anti β-actin (Santa Cruz, sc-47778)

B

SECONDARY ANTIBODIES
Alexa Fluor 488 goat anti-rabbit IgG (H+L) (Invitrogen)
Alexa Fluor 568 goat anti-mouse IgG (H+L) (Invitrogen)
Goat anti-mouse IgG (H+L)-HRP conjugate (Biorad, 172-1011)
Goat anti-rabbit IgG (H+L)-HRP conjugate (Biorad, 172-1019)

List of the primary (A) and secondary (B) antibodies used throughout the study.

2.4 Western Blotting

Cells were lysed in RIPA buffer (25mM Tris-HCl (pH 7.6), 150mM NaCl, 1%NP-40, 1% sodium deoxycholate, 0.1%SDS) containing 1x Halt Protease and Phosphatase Inhibitor Cocktail (Thermo Scientific). Lysates were maintained on ice for 20-30 minutes and then pipetted using a 21-½ G needle with 3ml syringe ten times to form homogenous lysates. Tubes were then centrifuged at 13,000g for 20 minutes at 4°C to clarify the supernatant of lysed proteins from undigested cellular constituents. Pellets were discarded and supernatants were kept on ice while protein concentrations were quantified using the BioRad Protein Assay (BioRad Laboratories) and read at 750nm on the 2800 UV/Vis Spectrophotometer by Unico. A standard curve was established by using a serial dilution series of known concentration of bovine albumin serum (BSA) then plotting the 'average blank-absorbance' for each BSA standard vs. its concentration in µg/ml.[52] The protein concentration of each sample was then calculated by using the equation x=128.2y/volume (x: protein concentration in volume of sample measured, y: absorbance at 750nm, volume: volume of sample measured). Lysate volumes corresponding to 25-30µg protein were resolved on either an 8% or 10% sodium dodecyl sulfate polyacrylamide gel (SDS-PAGE) gel depending on protein size being evaluated. 10µl of Precision Plus Protein™ Dual Color Standards (Biorad #161-0374) were loaded in the first well of each gel to be used as a molecular weight standard. A higher percentage gel leads to smaller pore size and is used to resolve smaller proteins. After electrotransferring the proteins from the gel to a nitrocellulose membrane, the membrane was blocked for 1 hour at room temperature or overnight at 4°C using 5% blocking buffer (5g dry milk in 100ml PBS/Tween). The nitrocellulose membrane was then incubated with appropriate concentrations of primary antibody in 5%

blocking buffer overnight at 4°C with continuous shaking. After washing 3 times with PBS/Tween for 5 minutes each wash, the membrane was incubated with the appropriate dilution of secondary antibody in 5% blocking buffer for an hour at room temperature followed by 3 washes, 15 minutes each. SuperSignal® West Pico Chemiluminescent Substrate (Thermo Scientific, 34077) is an enhanced chemiluminescent (ECL) substrate for detection of horse radish peroxidase activity from secondary antibodies and was added to the membrane for 1 minute.[53] Films were then developed using the Kodak X-OMAT 2000A Processor.

2.4.1 To Detect Endogenous SIRT6 Levels in HGPS Compared to Normal Fibroblasts. The samples tested included three different HGPS strains (AG11513, AG01972 and AG03199), an atypical HGPS strain (AG07493), and three normal cell strains (GM00969 and AG09602 dermal fibroblasts and BJ foreskin fibroblasts). Rabbit anti-SIRT6 primary antibody was used at a concentration of 1µg/ml in 5% blocking buffer and goat anti-rabbit IgG secondary antibody was diluted in 5% blocking buffer for a final concentration of 0.25µg/ml.

2.4.2 To Confirm Expression of Ectopic SIRT6 Following SIRT6 Infection of HGPS and Normal Fibroblasts. The samples tested included: AG01972 (PD20.5); AG01972+SIRT6 (PD20.5); AG11513 (PD18); AG11513+SIRT6 (PD20.5); GM00969 (PD27.5); and, GM00969+SIRT6 (PD27.5).

2.4.3 To Confirm Successful Induction of Progerin in Normal Fibroblasts after Inducing with Doxycycline. For this analysis, anti-progerin primary antibody (1µg/µl) diluted and goat anti-mouse IgG secondary antibody (0.25µg/ml) were used. Samples tested included: GM00969 PD19.5, HDF-progerin (no induction), HDF-progerin (1000ng/ml dox for 4 days), HDF-progerin

(750ng/ml dox for 8 days), HDF-progerin (750ng/ml dox for 14 days), AG11513 PD11.5, and AG11513 SIRT6 PD20.5.

2.4.4 To Test Whether Ectopic Progerin Expression Alone Reduces SIRT6 Protein Levels in Normal Fibroblasts. To determine whether the production of progerin affects the expression of SIRT6 protein, the following lysates were resolved by SDS-PAGE and immunoblotted with antibodies directed against SIRT6 as described above: GM00969 PD19.5, HDF-progerin (no induction), HDF-progerin (1000ng/ml dox for 4 days), HDF-progerin (750ng/ml dox for 8 days), HDF-progerin (750ng/ml dox for 14 days), AG11513 PD11.5, and AG11513 SIRT6 PD20.5.

2.4.5 To Test the Enzymatic Deacetylase Activity of SIRT6. Acetylated H3K9 levels were examined in HGPS and normal fibroblasts before and after ectopic SIRT6 expression. Samples tested included: GM00969 PD33, GM00969 SIRT6 PD28.5, AG11513 PD18, and AG11513 SIRT6 PD20.5. Mouse monoclonal anti-acetyl-Histone H3 (Ac-Lys^{9}) primary antibody (2µg/ml) and goat anti-mouse IgG secondary antibody (0.25µg/ml) were used.

β-actin, an abundantly expressed protein in all eukaryotic cells, was used as a loading control (0.2µg/ml) for all Western blot analyses.

2.5 Immunofluorescence (IF) staining

All samples were seeded as triplicates on acid-treated and ethanol sterilized coverslips at a density of 10^5 cells per 22x22mm coverslip (Fisher Scientific) in 6 well dishes. Cells were cultured overnight and the culture medium was then removed followed by one washing step with 2ml 1X Phosphate-Buffered Saline (PBS, Gibco). The cells were fixed by adding 2ml of fresh

3.7% paraformaldehyde for 10 minutes at room temperature (RT). The cells were washed 3 times in PBS, 5 minutes each washing step, then permeabilized using PBS + 0.1% Triton X-100 and incubated for 15 minutes at RT. The cells were washed three times in PBS, 5 minutes each and then blocked for 15 minutes using 2ml per well of blocking buffer, consisting of 1X PBS + 0.15% glycine + 1% BSA. Primary antibodies were diluted in blocking buffer to the appropriate concentration (1-2µg/ml) as recommended by the manufacturer. 50µl of diluted primary antibody was spotted onto parafilm and coverslips were added and placed in a humid container overnight at 4°C. Coverslips were returned to 6 well dishes to be washed three times, 10 minutes each wash in 1X PBS. Secondary antibody was diluted to its appropriate concentration and 50µl of diluted antibody was spotted on parafilm and coverslips placed on top. Coverslips were incubated for 45 minutes – 1 hour in the dark at RT followed by 3 washing steps, 3ml/well 1X PBS, 10 minutes each wash. 10µl of Vectashield® mounting medium for fluorescence with DAPI (1.5µg/ml DAPI) (Vector Laboratories, Inc.) was dropped onto each precleaned double frosted microscope slide (Fisher Scientific) for each coverslip containing immunolabeled cells. The blue-fluorescent DAPI allows for the visualization of nuclei as it specifically intercalates into DNA. Clear nail polish was used to seal the edges of the coverslips to avoid drying out. Slides were protected from the light at 4°C until images were captured at 40x and 100x objectives using the Nikon Eclipse E8000M fluorescence microscope and SPOT™ software.

100 nuclei for each sample was scored using Image J, the image processing and analysis application. The software scores the total number of foci in a given field and the average number of 53BP1 positive foci per nucleus was quantified by dividing the total number of foci

by the total number of nuclei. A uniform threshold value was set throughout all the samples to ensure consistent detection of foci.

2.5.1a To Determine the Extent of DNA Damage in HGPS Fibroblasts Compared to Normal Fibroblasts and as a Function of Replicative Age. The frequency of 53BP1-positive foci was analyzed in the following samples: Normal fibroblasts (GM00969 PD29, GM00969 PD41, and AG09602 PD17) and HGPS fibroblasts (AG11513 PD11.5 and AG11513 PD24). GM00969 PD29.5 + 0.75µM Adriamycin was used as a positive control. Positive controls for the presence of DNA double strand breaks (DSBs) were generated by acutely treating normal fibroblasts, GM00969, in the dark with culture medium containing 0.75 µM adriamycin for 2 hours. Adriamycin is an intercalative antitumor drug which when exposed to mammalian cells, induces DNA strand breaks, increased activity of p53 and senescence.[50,51] After 2 hours, culture media was replaced with fresh media and cells were left to recover for 24 hours before fixing for immunofluorescence. Mouse anti-53BP1 primary antibody was diluted in blocking buffer to a concentration of 0.8µg/ml and Alexa Fluor 568 secondary antibody was used at a concentration of 4µg/ml. Adriamycin emits a red fluorescence essentially in the same spectrum as Alexa 568, therefore, Adriamycin treated controls were stained with Alexa Fluor 488 secondary antibody to ensure any fluorescence emitted was solely due to the presence of 53BP1 foci. A negative control (GM00969 PD26.5) was included to support the validity of staining and identify the presence of any experimental artifacts. As a negative control, cells were incubated with the antibody diluent (1% BSA) without the primary antibody followed by incubation with labeled secondary antibodies.

2.5.1b To Determine Whether Ectopic SIRT6 Expression Mitigates DNA Damage in HGPS Cells. The frequency of 53BP1-positive foci was assessed in the following samples: AG11513 PD11.5 and AG11513 SIRT6 PD12using our standard protocol as described above.

2.5.2 SIRT6 Immunofluorescence

2.5.2a To Confirm the Initial Western Blotting Trend, Endogenous Levels of SIRT6 Protein in HGPS Fibroblasts Compared to Normal Fibroblasts Were Analyzed via IF Assay. SIRT6 levels were examined in AG11513 PD17 compared to GM00969 PD27 as well as a no primary antibody (GM00969) control. Samples were stained using rabbit anti-human SIRT6 primary antibody diluted in 1%BSA to a concentration of 10µg/ml and Alexa rabbit 488 secondary antibody (4µg/ml). The immunofluorescence assay was carried out as previously described (see section 2.5).

The intensity of SIRT6 staining was compared qualitatively among samples.

2.5.2b To Confirm SIRT6 Overexpression Following Lentiviral Infection. Following SIRT6 infections, levels of SIRT6 overexpression were assessed in the following samples: GM00969 PD32, GM00969 SIRT6 PD32.5, AG11513 PD16, AG11513 SIRT6 PD 23.5, and a no primary antibody control. Evidence of SIRT6 overexpression compared to uninfected samples was concluded qualitatively.

2.6 Senescence-Associated β-Galactosidase Activity Assay

Histochemical staining for SA-β-gal was used to detect senescent cells in HGPS (AG11513 PD10.5 and PD20.5) and normal (GM00969 PD21.5 and PD43, and AG09602 PD19 and PD32.5)

fibroblast cultures. Senescence was assessed in HGPS fibroblasts vs. normal fibroblasts as well as as a function of replicative age.

Each sample was seeded at subconfluency (ie. $1x10^5$ cells/6 well dish) in triplicate and the assay was performed at pH6.0 using the Senescence β-Galactosidase Staining Kit (Cell Signaling Technology, Inc.). As a positive control for senescence, GM00969 cells were exposed to 0.75μM Adriamycin for 2 hours and maintained in supplemented medium for 4 days prior to fixing.[51] The extent of senescence could was examined by comparing intensities of β-galactosidase histochemical staining and assessing cellular morphology to further support existence of a senescent state. During cellular senescence, fibroblasts change their morphology from a spindle shape to an enlarged, flattened, and irregular shape.

2.7 Quantitative Real-Time Polymerase Chain Reaction (qRT-PCR)

To detect levels of endogenous SIRT6 mRNA in HGPS fibroblasts relative to GM00969 fibroblasts, cells were collected at 70% confluency and RNA for each sample was isolated with the SV Total RNA Isolation System (Promega) according to the manufacturer's protocol. 1μg of RNA was reverse transcribed using the High-Capacity cDNA Reverse Transcription kit (Applied Biosystems). The thermal cycler (PTC-100 Programmable Thermal Controller, MJ Research,Inc.) was programmed using the following conditions: 25°C for 10 minutes, 37°C for 120 minutes, 85°C for 5 minutes and then a 4°C 'soak' until the samples were retrieved. 20μl (1μg) of reverse transcription reaction for each sample was used for qRT-PCR using primers for SIRT6 (forward, 5'-CCCACGGATCTGGACCA; reverse, 5'-CTCTGCCAGTTTGTCCCTG) and endogenous control,

cyclophilin A (PPIA) (forward, 5'-GCATGATCGGGAGGGTTTACT; reverse, 5'-TCCTTGCCACTCCTATTCCTT). PPIA is a cytosolic and moderately abundant protein that functions in cellular protein folding and protein interactions. Its stable expression allows for the quantification of the gene of interest by comparing the gene expression to this internal standard.[55] All reactions were carried out in triplicate on the ABI 7900HT Fast Real-Time PCR System. SIRT6 expression levels were calculated by relating mean cycle threshold (C_t) ± SD of triplicates values to the mean values of the endogenous control, PPIA.[55]

2.8 Cell Proliferation

Proliferation rates of HGPS fibroblasts were compared to those of normal fibroblasts from young and old donors. Proliferation rates were also assessed as a function of replicative age (low vs. high population doublings). The parameter used to assess proliferation rates was the population doubling time (PDT), which is the time taken for the culture to increase twofold in the middle of the exponential phase of growth. The PDTs were assessed as follows: in a 12-well plate, each sample was seeded in triplicates for each time point i.e. 24, 48 and 72 hours. After 24hrs, the first plate was trypsinized with 0.2ml trypsin, incubated for 5 minutes followed by the addition of 0.2ml medium (total volume 0.4ml). The cells were then counted in each of the three wells using a hemocytometer. Sampling was repeated at 48 and 72hrs. A fourth well for each sample was seeded and stained with methylene blue (0.2% methylene blue + 50% methanol/deionized H_2O) at each time point to assess uniform distribution of cells in the wells and qualitatively compare rates of cell growth with time.

Number of cells/well = Average number of cells counted x volume of trypsin+media used (ml) x 10^4

The doubling time was then calculated using the software http://www.doubling-time.com. The equation for calculating doubling time is:

Doubling time (hours) = t x log2 / $logN_t$ *-* $logN_o$

Where t: time period; N_t: number of cells at time t; N_o: initial number of cells.

The average doubling times and standard error from each replicate were then calculated.

2.11 Statistical Analysis

Data was analyzed using 2-tailed Student's *t* test and a *P* value less than 0.05 was considered significant.

3 RESULTS

3.1 HGPS fibroblasts express lower levels of SIRT6 protein than normal fibroblasts, which positively correlates with DNA damage, β-galactosidase positivity and reduced proliferative capacity.

3.11 HGPS Fibroblasts Express Lower Endogenous Levels of SIRT6 than Normal Fibroblasts.

In a previous study, the generation of *Sirt6*$^{-/-}$ mice resulted in mice with multiple shared phenotypes of those with Hutchinson-Gilford Progeria Syndrome.[42] The levels of SIRT6 protein have not been examined in HGPS fibroblasts, therefore**, I first hypothesized that HGPS fibroblasts express lower levels of SIRT6 protein than normal fibroblasts**. 3 different HGPS strains (AG11513, AG01972 and AG03199), an atypical HGPS strain (AG07493), and three normal cell strains (GM00969 and AG09602 dermal fibroblasts and BJ foreskin fibroblasts) were assessed for progerin and SIRT6 expression. As expected, Western analysis revealed that only typical HGPS cells (AG11513, AG01972 and AG03199) expressed progerin (Figure 5A). SIRT6 expression was noticeably reduced in the HGPS strains compared to normal fibroblasts (Figure 5B). It also worth noting that typical HGPS strains expressed lower SIRT6 levels than the atypical HGPS strain.

To confirm these findings, typical HGPS (AG11513 PD17) and normal fibroblasts (GM00969 PD27) of young replicative ages were immunolabeled with anti-SIRT6 primary antibody

followed by anti-rabbit Alexa 488 secondary antibody in an immunofluorescence assay. AG11513 nuclei displayed much weaker signal intensity when compared to GM00969, indicating reduced SIRT6 protein in the HGPS nuclei (Figure 5D).

To determine whether SIRT6 was also reduced at the transcriptional level in HGPS cells, RNA was isolated from normal fibroblasts, an atypical HGPS strain, and a typical HGPS strain. qRT-PCR was conducted using primers for *SIRT6* and the endogenous control, PPIA. The reactions were carried out in triplicate and mRNA levels were normalized to the endogenous control. mRNA levels of SIRT6 in the atypical and typical HGPS strains mirrored the protein levels observed in the Western blot. Although statistically insignificant, atypical, and to a greater extent, typical HGPS strains expressed lower levels of SIRT6 mRNA when compared to a normal fibroblast (GM00969) control (Figure 5C).

Collectively, these results indicate that typical HGPS fibroblasts express lower levels of SIRT6 than normal fibroblasts and that SIRT6 expression may be at least in part regulated at the transcriptional level. Atypical HGPS fibroblasts exhibit higher levels of endogenous SIRT6 than typical HGPS fibroblasts, which could be attributed to their lack of progerin production.

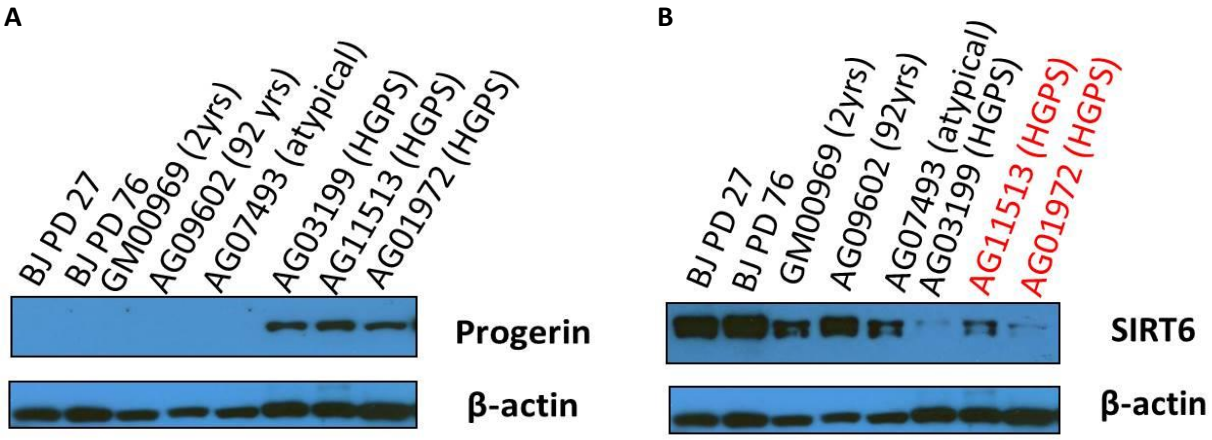
A
BJ PD 27
BJ PD 76
GM00969 (2yrs)
AG09602 (92 yrs)
AG07493 (atypical)
AG03199 (HGPS)
AG11513 (HGPS)
AG01972 (HGPS)
Progerin
β-actin
B
BJ PD 27
BJ PD 76
GM00969 (2yrs)
AG09602 (92yrs)
AG07493 (atypical)
AG03199 (HGPS)
AG11513 (HGPS)
AG01972 (HGPS)
SIRT6
β-actin

C

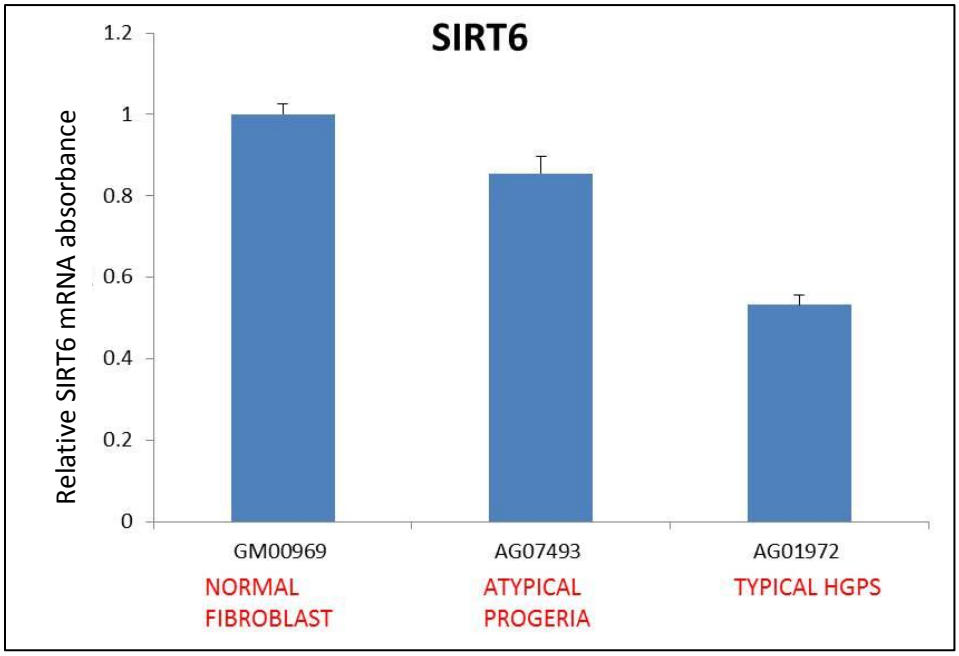
SIRT6
Relative SIRT6 mRNA absorbance
1.2
1
0.8
0.6
0.4
0.2
0
GM00969
AG07493
AG01972
NORMAL FIBROBLAST
ATYPICAL PROGERIA
TYPICAL HGPS

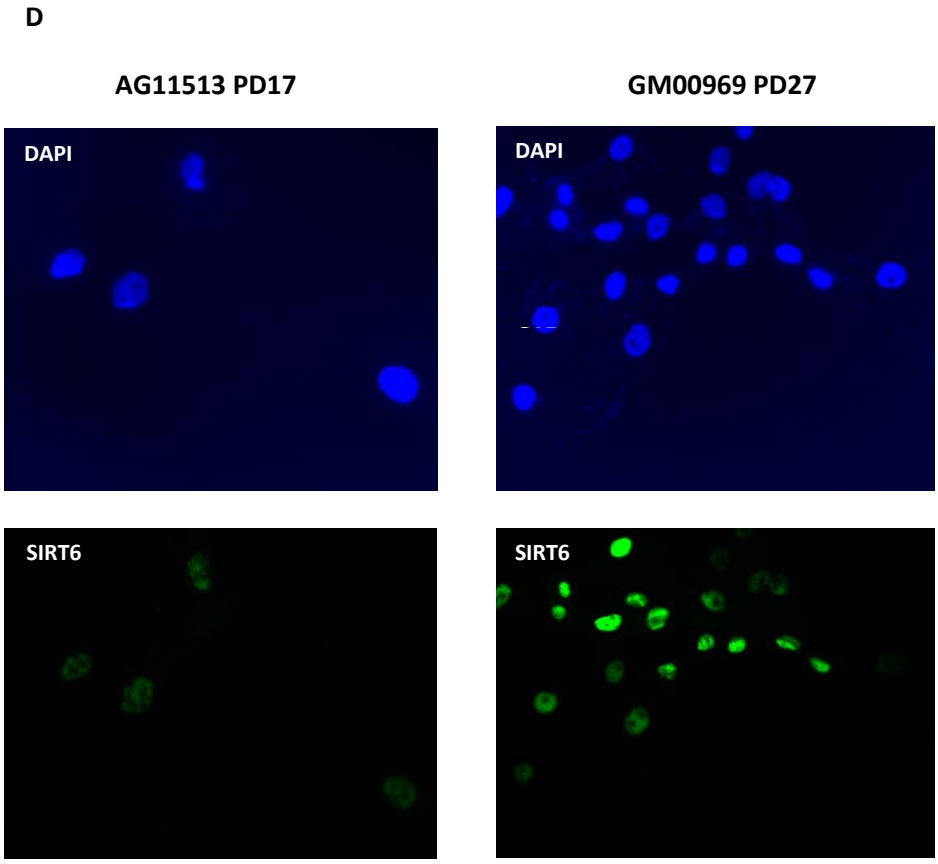

Figure5. Assessment of endogenous SIRT6 levels in HGPS and normal fibroblasts. (A) Western analysis to characterize typical HGPS strains by their expression of the mutant protein progerin, the result of a single nucleotide mutation (G608G) in exon 11 of the *LMNA* gene. Unlike atypical HGPS fibroblasts and normal fibroblasts, typical HGPS strains AG03199, AG11513 and AG01972 express progerin. (B) Typical HGPS strains express markedly lower levels of SIRT6 protein than atypical HGPS and normal fibroblasts. Blots were probed first with progerin, and then sequentially reprobed for SIRT6 and β-actin (loading control). (C) Quantitative RT-PCR was used to detect mRNA levels of endogenous SIRT6 expression in AG07493 and AG01972 fibroblasts. Relative quantities were normalized to *PPIA*. AG01972 fibroblasts expressed about 47% less SIRT6 mRNA than normal fibroblasts while AG07493 fibroblasts only 15% less. Error bars represent SD of replicates. (D) Representative immunofluorescence images of AG11513 and GM00969 cells at a 40X magnification. SIRT6 is stained in green and nuclei, stained with DAPI, in blue.

Low levels of SIRT6 were observed specifically in progerin-expressing fibroblasts. So does the expression of progerin alone have an effect on the levels of SIRT6 protein expressed, or are other factors specific to HGPS cells responsible for the relatively lower SIRT6 levels? To answer this question, human diploid fibroblasts (HDF) transfected with an EGFP-progerin construct were treated with doxycycline to induce progerin production and the levels of SIRT6 protein were analyzed (Figure 6). HDFs that were not induced by doxycycline to produce progerin did not express detectable progerin protein when probed with anti-progerin antibody (Figure 6A). Only after exposing the fibroblasts to 1000ng/ml doxycycline for 4 days, cells produced an abundance of progerin indicating a tightly regulated inducible system (Figure 6B). An exaggerated level of progerin protein in HDFs resulted in a down-regulation of SIRT6 protein. However, when progerin was expressed at levels similar to HGPS fibroblasts, no effect was seen on SIRT6 expression. There was also no effect on SIRT6 protein levels with increasing time of progerin production in culture.

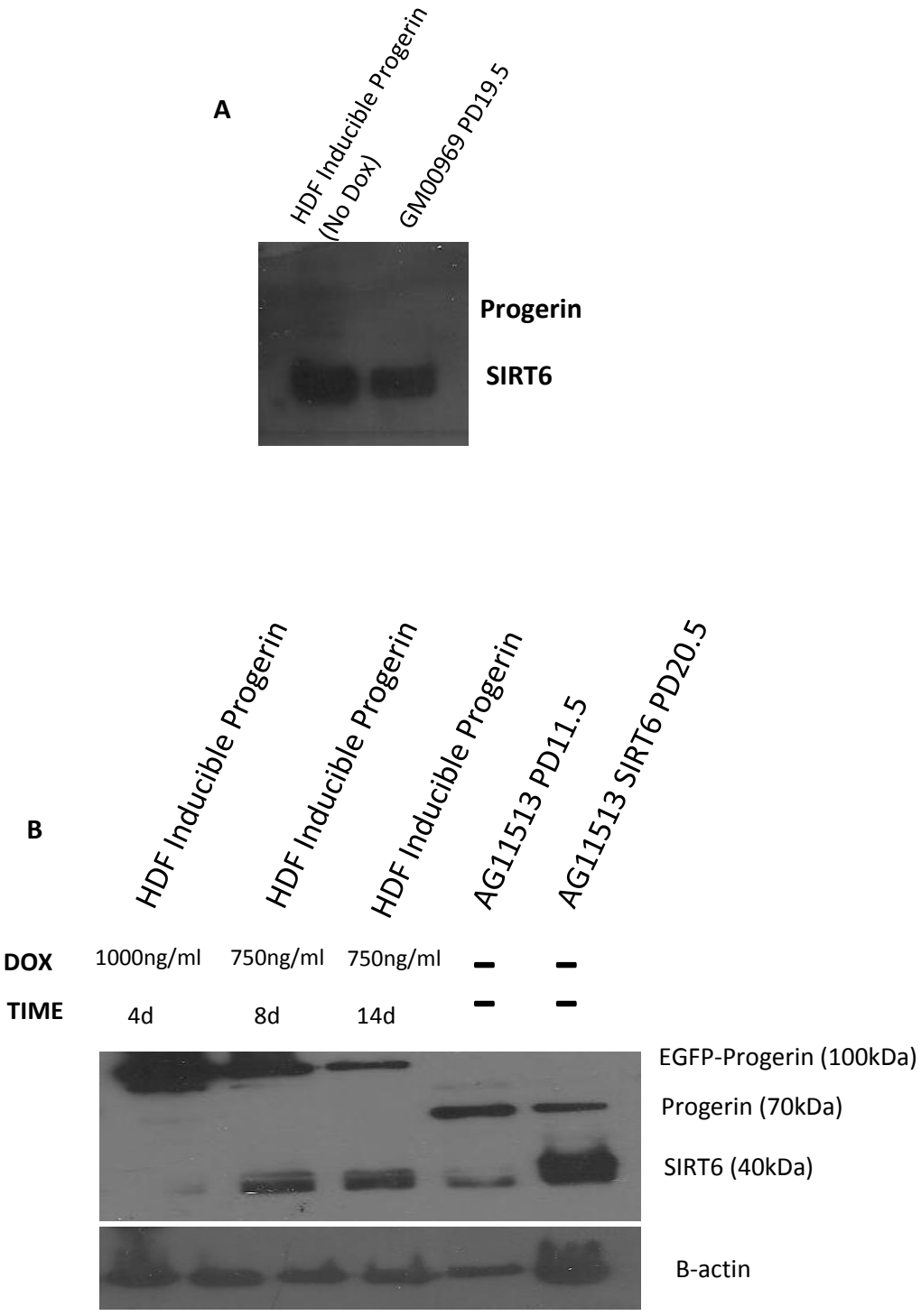

Figure 6. Effect of Progerin Production on SIRT6 Protein Expression. *(A)* Western Blot showing endogenous SIRT6 and progerin levels in HDF without doxycycline treatment and GM00969 normal fibroblasts. *(B)* Western Blot showing the effect of progerin production on SIRT6 levels. Induced progerin is tagged to EGFP and has a higher molecular weight (~100 kDa) than

endogenous progerin (70kDa) expressed by HGPS fibroblasts. An exaggerated level of progerin protein in HDFs resulted in a downregulation of SIRT6 protein. However, when progerin was expressed at levels similar to HGPS fibroblasts, no effect was seen on SIRT6 expression. There was no effect on SIRT6 protein levels with increasing time of progerin production in culture.

3.12 HGPS Fibroblasts Exhibit a Higher Frequency of 53BP1 Foci than Normal Fibroblasts.

DNA damage in the form of DNA double-strand breaks (DSBs) can be assessed by the presence of 53BP1 (p53-binding protein 1) foci. 53BP1 is one of the mediators of the DNA damage repair pathway following the detection of DSBs and is required for the phosphorylation of p53, which ultimately leads to cell cycle arrest.[36] If the DNA damage is reversible, p53 activity decreases after quick repair, however, when repair is slow or incomplete p53 activity is sustained. A higher frequency of 53BP1 foci corresponds to a greater number of unrepaired DSBs. An immunofluorescence assay was used to analyze the frequency of 53BP1 foci in HGPS fibroblasts compared to normal fibroblasts (Figure 7D-G). The average frequency of 53BP1-positive foci per nucleus was determined in AG11513 PD11.5 and PD24, GM00969 PD29 and PD41, AG09602 PD17, and GM00969 PD29.5 acutely treated with adriamycin for 2 hours (positive control). Cells were seeded in triplicate and stained with mouse anti-53BP1 primary antibody followed by Alexa Fluor 568 (red) secondary antibody. The nuclei of adriamycin-treated cells, without being probed for Alexa Fluor 568 secondary antibody, emit red fluorescence due to the accumulation of the chemotherapeutic drug and were therefore probed with Alexa Fluor 488 (green) secondary antibody (Figure 7A,B).

100 nuclei from each replicate were scored for all of the samples using Image J. A uniform threshold value was set across all samples where a focus was only scored if it was above the

minimum threshold value. The average frequencies of 53BP1-positive foci ± SD of replicates were then graphed for each sample (Figure 7H). Approximately 21 foci per nucleus were seen for the positive control sample. AG11513 (PD11) fibroblasts showed 5.9 foci per nucleus, which was not significantly higher than normal GM00969 (PD29) fibroblasts (5.2 foci per nucleus) (p-value= 0.7). However, the 18 PD difference between samples should be taken into account. AG09602 PD17 (92 year old donor) had a significantly higher frequency of 53BP1 foci compared to GM00969 PD29 (2 year old donor) fibroblasts (p-value=0.00135). For both GM00969 and AG11513 fibroblasts, there was no significant difference in the number of 53BP1 foci with increasing replicative age (p-values= 0.87 and 0.18, respectively). Together, these results indicate that HGPS fibroblasts at a relatively young replicative age (PD11) display a level of DNA damage similar to normal fibroblasts at a much older population doubling (PD29). These results along with findings in the literature[56] suggest that with age, there is a decreasing efficiency in DNA repair as indicated by the abundant presence of DNA damage-induced foci of 53BP1. Additionally, no significant increase in the number of 53BP1 foci was observed in 2 year old normal fibroblasts with increasing replicative age suggesting that the occurrence of DSBs may not increase with increasing time in culture in young normal fibroblasts, or perhaps the cells were not aged long enough. However, AG11513 fibroblasts showed a gradual increase in the frequency of 53BP1 foci with increasing replicative age with approximately 6 foci per nucleus at PD11.5 (p-value=0.7) and 8 foci per nucleus at PD24 (p-value=0.18). Continuing to age the HGPS cells further may show a significant increase in the incidence of DSBs.

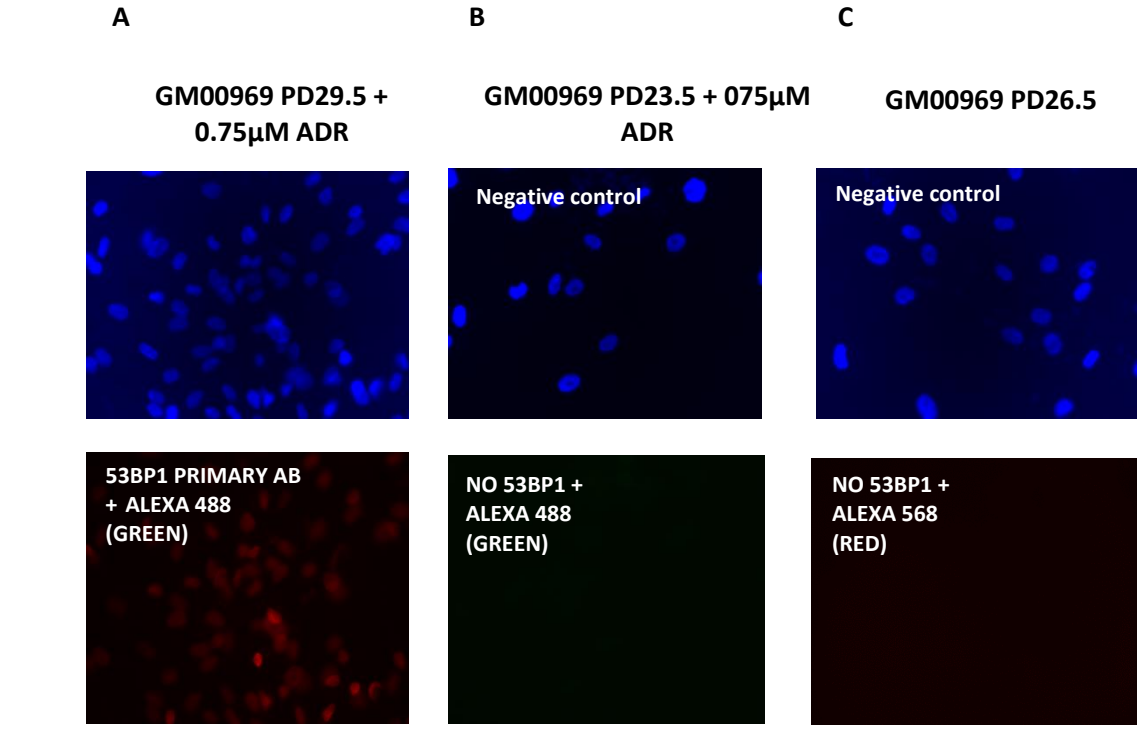
A
B
C
GM00969 PD29.5 + 0.75µM ADR
GM00969 PD23.5 + 075µM ADR
GM00969 PD26.5
Negative control
Negative control
53BP1 PRIMARY AB + ALEXA 488 (GREEN)
NO 53BP1 + ALEXA 488 (GREEN)
NO 53BP1 + ALEXA 568 (RED)

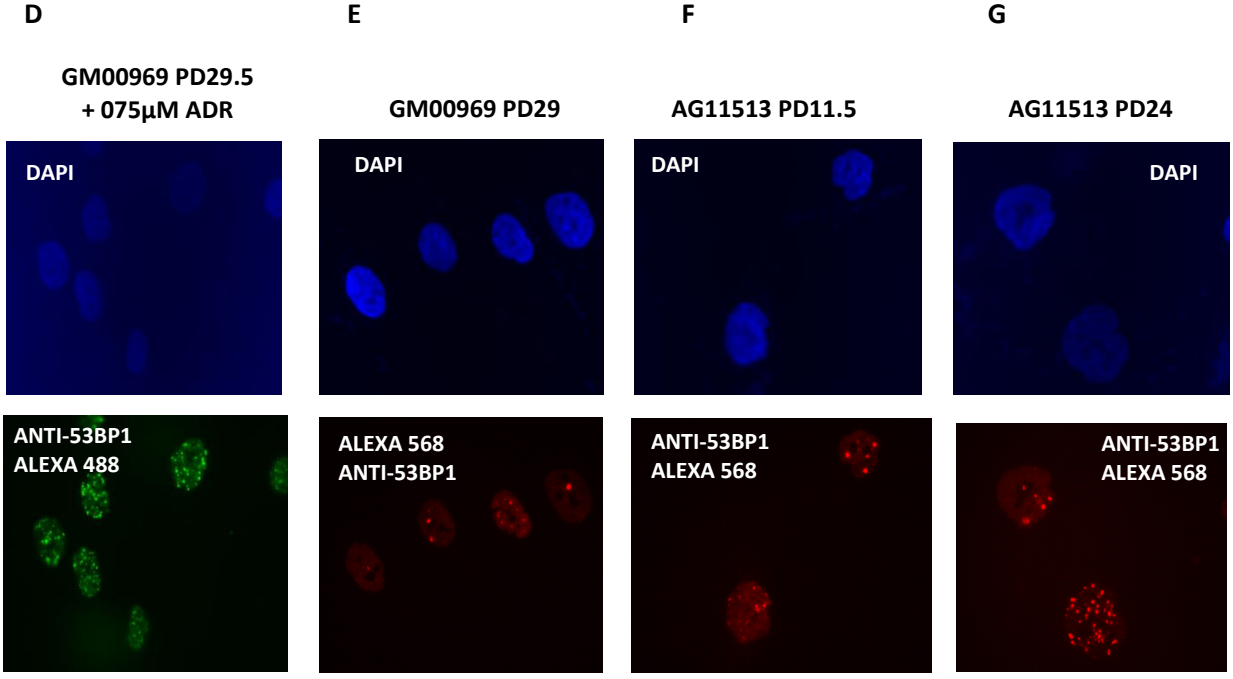
D
E
F
G
GM00969 PD29.5 + 075µM ADR
GM00969 PD29
AG11513 PD11.5
AG11513 PD24
DAPI
DAPI
DAPI
DAPI
ANTI-53BP1 ALEXA 488
ALEXA 568 ANTI-53BP1
ANTI-53BP1 ALEXA 568
ANTI-53BP1 ALEXA 568

H

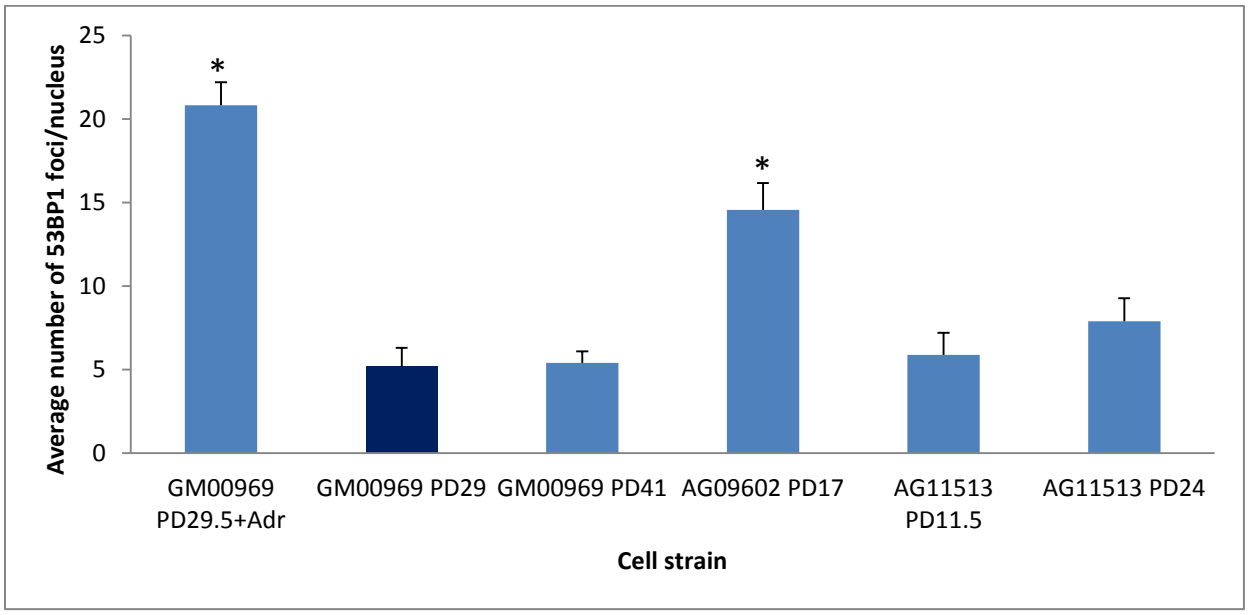

Figure 7. Incidence of DSBs Represented By Frequency of 53BP1 Foci. *(A)* Representative immunofluorescence images of no primary antibody negative controls. Adriamycin-treated cells emit red fluorescence without Alexa 568 (red) secondary antibody. *(B)* No primary antibody negative control for Adriamycin-treated cells with Alexa 488 (green) secondary antibody. *(C)* No primary antibody negative control for GM00969 cells with Alexa 568 (red) secondary antibody. Images were taken at a 40X magnification and nuclei were stained blue with DAPI. Representative images displaying 53BP1 foci at 100X magnification of GM00969+0.75µM Adr *(D),* GM00969 PD29 *(E)*, AG11513 PD11.5 *(F)*, and AG11513 PD 24 *(G)*. *(H)* Bars represent the frequency of 53BP1 foci per nucleus in each sample. Data were derived from three independent experiments. Error bars represent standard error (SE) of replicates. For each sample the p value was compared to GM00969 PD29. Statistically significant results have a p value less than 0.05 (*$p<0.05$).

3.13 HGPS Fibroblasts Senesce Prematurely Compared to Normal Fibroblasts.

Senescence-associated β-Galactosidase (SA β-gal) was used as a biomarker to qualitatively assess the senescence in HGPS fibroblasts compared to normal fibroblasts from young (GM00969) and old (AG09602) donors. We had hoped to determine the frequency of β-gal

positivity but were unable due to limitations of using this assay (see discussion). A widespread histochemical staining reaction together with the adoption of an enlarged and flattened cellular morphology, were collectively highly consistent with a senescent state. Fibroblasts stained using SA β-Gal included: GM00969 PD21.5 and PD43, AG09602 PD19 and PD32.5, and AG11513 PD10.5 and PD20.5. Using this assay allows us to qualitatively examine the premature senescence seen in HGPS fibroblasts. GM00969 and AG09602 at young PDs exhibited slight staining, (possibly background staining) however, they still displayed the typical fusiform-cell morphology shared by low passage fibroblasts (Figure 8B-E). Conversely, AG11513 HGPS fibroblasts at a young PD of 10.5 had a more flattened, irregular shaped morphology with darker staining comparable to the positive control. The senescent phenotype of the AG11513 fibroblasts was more pronounced with older replicative age (PD20.5) (Figure 8F-G).

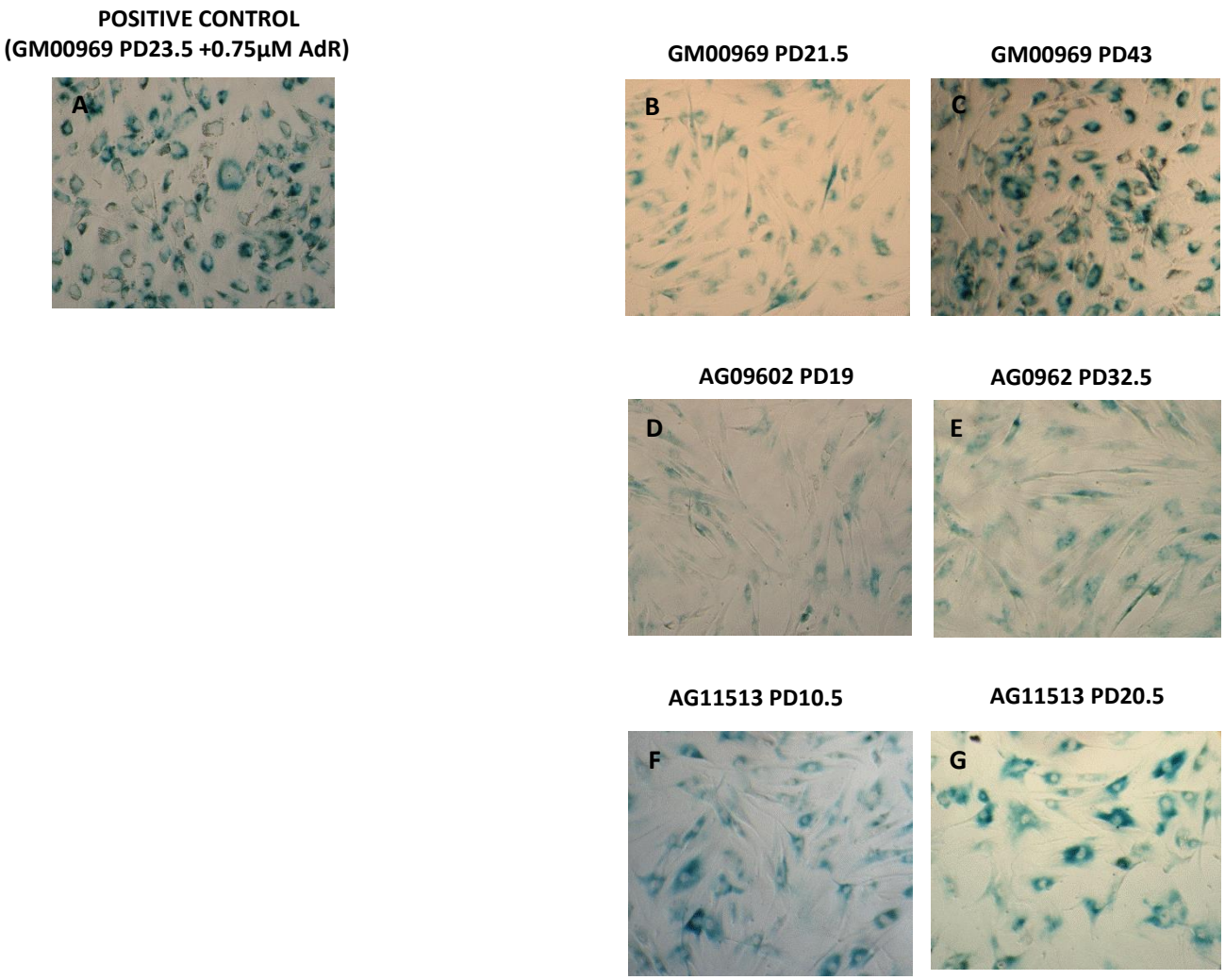

Figure 8. Senescence-Associated β-gal Staining in Cultured Fibroblasts. Images were captured at 20X magnification. *(A)* To induce senescence, GM00969 fibroblasts were acutely treated with 0.75µM Adriamycin for 2 hours. Fresh medium was then added and cells remained in culture for 4 days before fixing and staining. *B,D,F:* early passage fibroblasts; *C,E,G:* late passage fibroblasts. Late passage AG11513 fibroblasts displayed a flattened senescent morphology with darker histochemical staining.

3.14 HGPS Fibroblasts Have a Longer Doubling Time than Normal Fibroblasts and Doubling Time Lengthens with Increasing Replicative Age.

The proliferation rates of HGPS fibroblasts and normal fibroblasts were assessed via doubling times (Figure 9). Young AG11513 fibroblasts (PD12.5) had a slightly higher doubling time (49.7± 4.5 hours) than GM00969 fibroblasts (38.7 ± 2.97 hours), however this was not statistically significant (p-value=0.11). Both HGPS strains, AG11513 and AG01972, had significantly higher doubling times than normal fibroblasts of similar PD (p-value= 0.03 and 0.04, respectively) and doubling time increased with increasing replicative age (AG11513 PD12.5 to PD20 (p-value=0.07). Additionally, there was a significant increase in the doubling times of normal fibroblasts as replicative age increased from PD23.5 to PD40.5 (p-value=0.04).

.

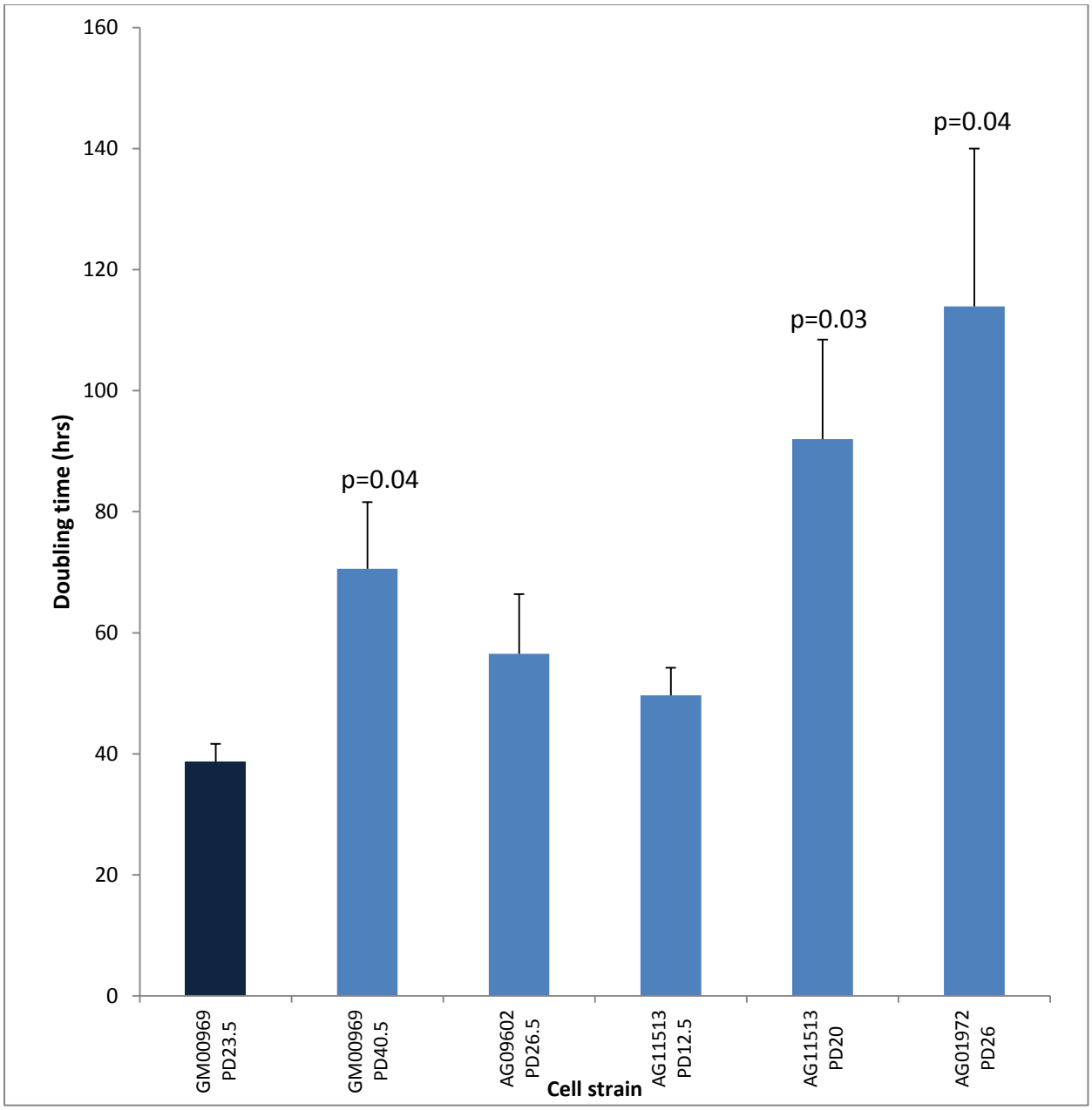

Figure 9. Proliferation Rates of HGPS and Normal Fibroblasts as a Function of Replicative Age. Bars represent the doubling time (hours) of each cell strain. For each sample, the replicate values for doubling time were compared to GM00969 PD23.5 (dark blue bar). At comparable population doublings, AG11513 fibroblasts (PD20) had a significantly higher doubling time (137.8%) than GM00969 fibroblasts (PD23.5) (p-value=0.03). Another HGPS strain (AG01972 PD26) had almost triple the doubling time of normal fibroblasts albeit being 14.5 PDs younger. With increasing replicative age, population doubling times of normal and HGPS fibroblasts approximately doubled.

Results from Aim 1 of this study uncovered a novel finding that typical (progerin-expressing) HGPS fibroblasts express lower levels of SIRT6 protein and mRNA than normal fibroblasts and even atypical HGPS fibroblasts. The expression of progerin alone did not seem to have a direct effect on the protein levels of SIRT6. Via the evaluation of 3 markers of cellular senescence, HGPS fibroblasts were found to exhibit more DNA damage than normal fibroblasts, display a pronounced senescent cellular morphology at young PDs, and have a longer population doubling time than normal fibroblasts at an equal or higher PD. On these grounds, it would be of great interest to examine whether SIRT6 overexpression in HGPS fibroblasts will prevent the premature senescence, a major contributing factor to this accelerated aging phenotype. The second half of this study aims to answer this question

3.2 Overexpressing SIRT6 Protects HGPS fibroblasts From DNA Damage, Premature Senescence and Slow Proliferation Rates.

SIRT6 has been found to be crucial in maintaining a normal replicative lifespan and preventing premature senescence in human fibroblasts.[44] $SIRT6^{-/-}$ in cells results in a shortened replicative lifespan and increased levels of SA-β-gal staining. Furthermore, SIRT6 has also been implicated in DNA repair since SIRT6 depletion has been linked to an increased frequency of phosphorylated γH2AX DNA damage foci.[44] Comparable cellular defects exist between $SIRT6^{-/-}$ and HGPS fibroblasts. Additionally, the aforementioned study demonstrating the abnormalities of SIRT6-deficient mice which overlap with progeroid pathologies[42], along with the study showing that male mice overexpressing SIRT6 have a significantly longer lifespan than wild-type

mice[42], have collectively led to the proposal that **overexpressing SIRT6 in HGPS fibroblasts may prevent the senescence-associated phenotypes in HGPS fibroblasts.**

The first objective of Aim 2 was to stably overexpress SIRT6 in HGPS and normal fibroblasts using a lentiviral vector. The lentiviral vector (pCDH-CMV-MCS-EF1-Puro) was chosen as it offers stable, efficient and long-term expression of the target gene in almost any mammalian cell including those that are post-mitotic. Owing to the poor proliferation capacity of HGPS cells, this lentivector construct was the delivery vehicle of choice. An empty vector control was used to develop a controlled system to exclusively examine the effects of SIRT6 overexpression in HGPS and normal fibroblasts. After 5 days of puromycin treatment, to select for cells successfully expressing the lentiviral vector, cells carrying the empty vector grew poorly compared to their SIRT6-overexpressing and uninfected parental counterparts (Figure 10 A-C). Unfortunately, we were unable to expand sufficiently for subsequent comparable analyses with SIRT6 overexpressing cells. As a result, uninfected cells were used as controls. SIRT6 was overexpressed in 2 different HGPS strains (AG01972 PD10 and AG11513 PD11) and one normal strain (GM00969 PD25) as indicated by Western blotting analysis (Figure 10D) and confirmatory immunofluorescence assay verifies that SIRT6 overexpression was nuclear in cellular localization (Figure 10E-H).

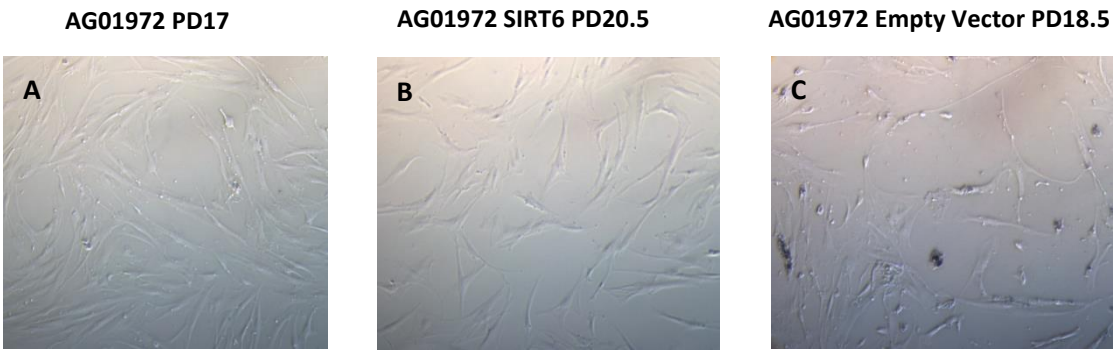
AG01972 PD17
AG01972 SIRT6 PD20.5
AG01972 Empty Vector PD18.5
A
B
C

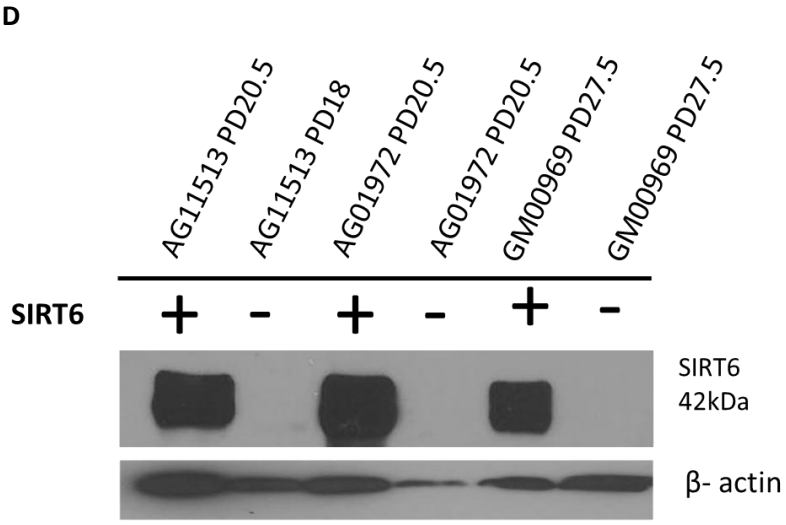
D
AG11513 PD20.5
AG11513 PD18
AG01972 PD20.5
AG01972 PD20.5
GM00969 PD27.5
GM00969 PD27.5
SIRT6
+ - + - + -
SIRT6
42kDa
β- actin

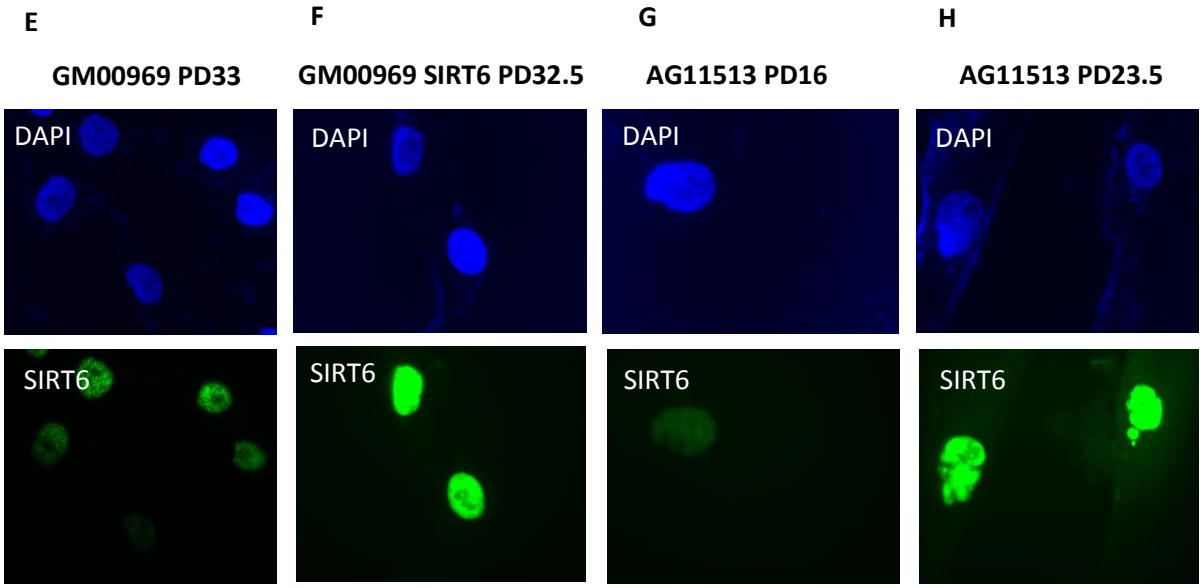
E
F
G
H
GM00969 PD33
GM00969 SIRT6 PD32.5
AG11513 PD16
AG11513 PD23.5
DAPI
DAPI
DAPI
DAPI
SIRT6
SIRT6
SIRT6
SIRT6

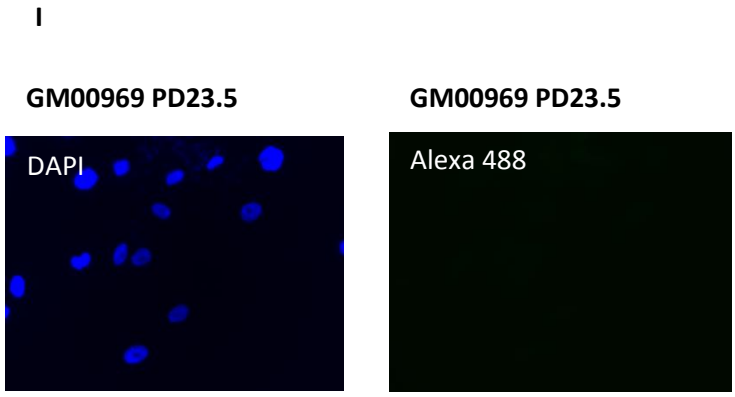

Figure 10. SIRT6 Overexpression in HGPS and Normal Fibroblasts. Representative bright-field images of *(A)* Uninfected parental AG01972 PD17, *(B)* AG09172+SIRT6 PD20.5, *(C)* AG01972+empty vector PD18.5. The same outcome was seen with AG11513+empty vector (Images not shown). Image *(C)* showing cellular debris and unhealthy, dying fibroblasts compared to *(A)* and *(B)*. Images captured at 20x magnification under a phase-contrast microscope. *(D)* Western blot analysis of SIRT6 overexpression in AG11513, AG01972 and GM00969 fibroblasts. *E-H:* Representative immunofluorescence images showing nuclear specific SIRT6 overexpression. Fibroblasts overexpressing SIRT6 show a visibly more intense signal than their uninfected counterparts. Cells were immunostained with antibodies against SIRT6 and Alexa 488 and counterstained with DAPI. Images were captured at 100x magnification. (*I)* No primary antibody (SIRT6) negative control at 40x magnification.

3.21 SIRT6 Overexpression Reduces the Occurrence of DNA-Damage Induced DSBs.

As shown in Figure 11, overexpressing SIRT6 in AG11513 HGPS fibroblasts resulted in a significant and dramatic reduction in the frequency of 53BP1 foci (p-value= 0.01). AG11513 HGPS fibroblasts displayed 5.87 53BP1-positive foci per nucleus while AG11513 fibroblasts overexpressing SIRT6 reduced this frequency to about 2.5.

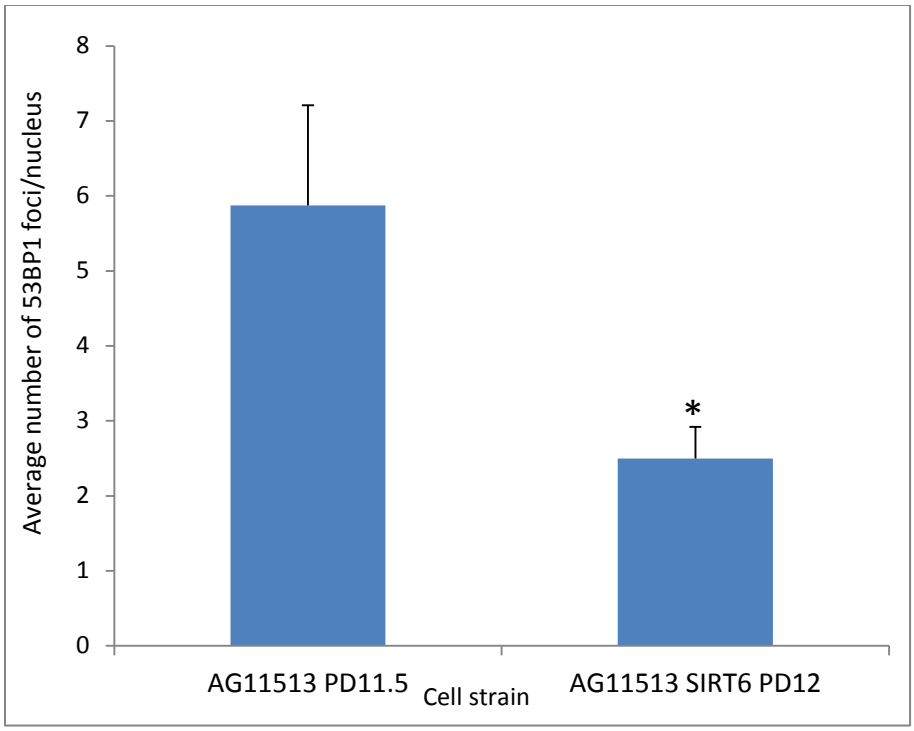

Figure 11. Incidence of DSBs represented by frequency of 53BP1 foci ± SIRT6. Bars represent the frequency of 53BP1 foci per nucleus in AG11513 fibroblasts ± SIRT6. Data were derived from three independent experiments. Error bars represent standard error (SE) of replicates. The p value was of AG11513 SIRT6 was compared to the uninfected AG11513 control. Statistically significant results have a p value less than 0.05 (*p<0.05).

3.22 SIRT6 Overexpression Delays Replicative Senescence in HGPS Fibroblasts.

SA β-gal activity was used in order to determine whether SIRT6 overexpression prevents the premature senescent phenotype of HGPS fibroblasts (Figure 12). AG11513 PD20.5 fibroblasts have a more flattened, irregular, senescent morphology compared to the same strain at PD10.5. However, AG11513 SIRT6 fibroblasts still showed a healthy, spindle-like morphology at PD20.5. Consistent results were seen when this assay was repeated in an independent experiment (images not shown).

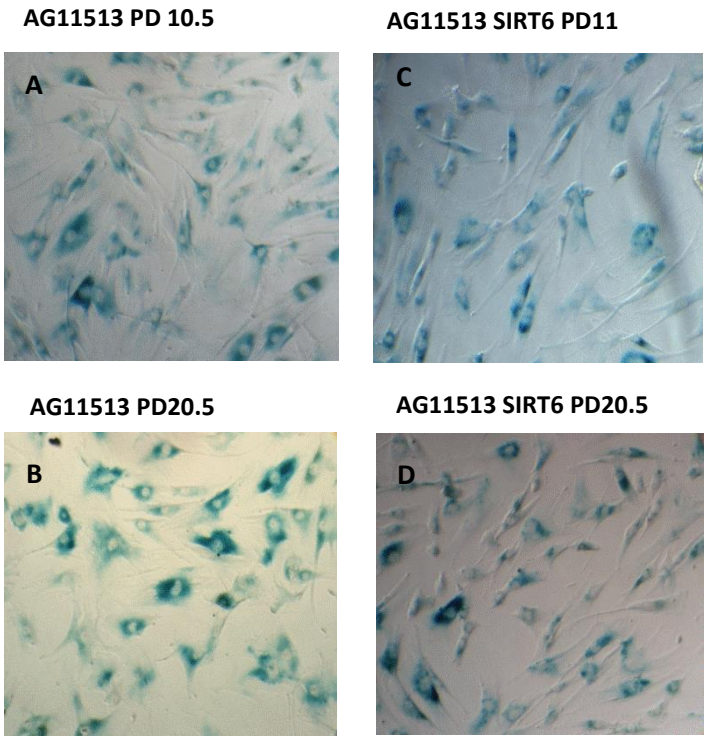

Figure 12. Senescence-Associated β-gal Staining in Cultured Fibroblasts. $1.5x10^4$ cells were seeded in triplicates in a 48-well dish and stained with β-gal staining solution 24 hours after plating. *(A,B)* Representative images of AG11513 PD10.5 and PD20.5 and *(C,D)* AG11513 SIRT6 PD11 and PD20.5 were captured at 20X magnification.

3.23 SIRT6 Overexpression Improves the Proliferative Capacity of HGPS Fibroblasts.

Since HGPS fibroblasts have significantly longer doubling times than normal fibroblasts, the proliferative capacity of HGPS fibroblasts overexpressing SIRT6 was examined. The PD times of AG11513 (PD12.5), AG11513 SIRT6 (PD12), AG11513 (PD20) and AG11513 SIRT6 (PD18.5) were assessed. Results showed that ectopic expression of SIRT6 significantly reduced doubling times compared to uninfected controls (AG11513 PD12.5 vs. AG11513 SIRT6 PD12 (p-value=0.04) and AG11513 PD20 vs. AG11513 SIRT6 PD18.5 (p-value=0.04)). Furthermore, as HGPS fibroblasts

aged in culture their doubling time dramatically increased (p-value=0.06), however, the increase in doubling time was much less pronounced in HGPS fibroblasts overexpressing SIRT6 (p-vaule=0.33).

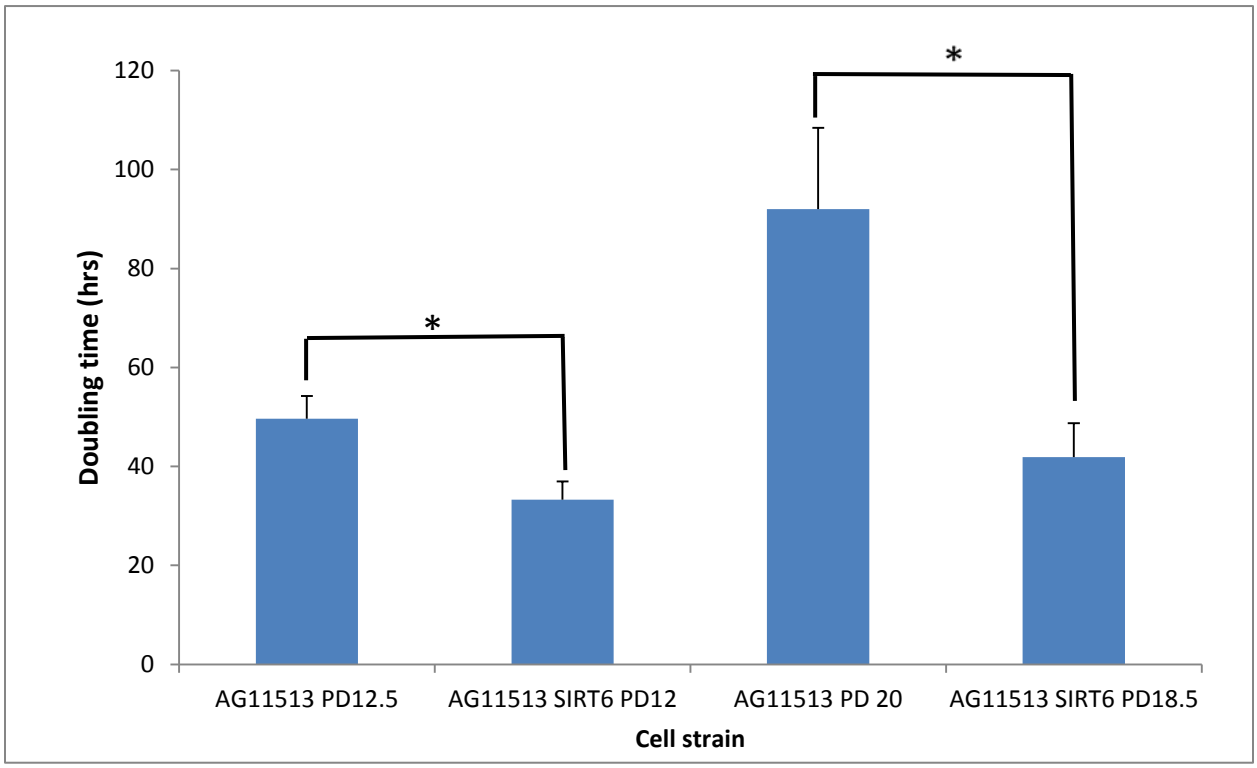

Figure 13. Proliferation Rates of AG11513 Fibroblasts ± SIRT6 Overexpression and as a Function of Replicative Age. Bars represent the doubling time (hours) of each sample. The doubling times of AG11513 SIRT6 were compared to parental AG11513 strains at comparable PDs. At early and late PDs, SIRT6 overexpression led to a significant reduction in the doubling times of HGPS fibroblasts (p-value=0.04). Statistically significant results have a p value less than 0.05 (*p<0.05).

3.3 The Beneficial Effects of SIRT6 Overexpression on Cellular Senescence May Be Specific to HGPS Fibroblasts.

To determine whether the effects of SIRT6 overexpression on the biological endpoints examined is specific to HGPS fibroblasts or has the same effect on normal fibroblasts, DNA damage, β-gal positivity, and proliferative capacity were assessed in GM00969 normal fibroblasts overexpressing SIRT6.

Preliminary results indicated that there was no significant difference in the average number of 53BP1 foci per nucleus (p-value=0.58) (Figure 14A). Results from the SA-β-gal assay also showed no noticeable difference in staining intensities or the cellular morphology (Figure 14B). Finally, although slightly shorter, the population doubling time of GM00969 SIRT6 fibroblasts was not significantly reduced when compared to the uninfected parental control (GM00969 PD 23.5) (Figure 14C).

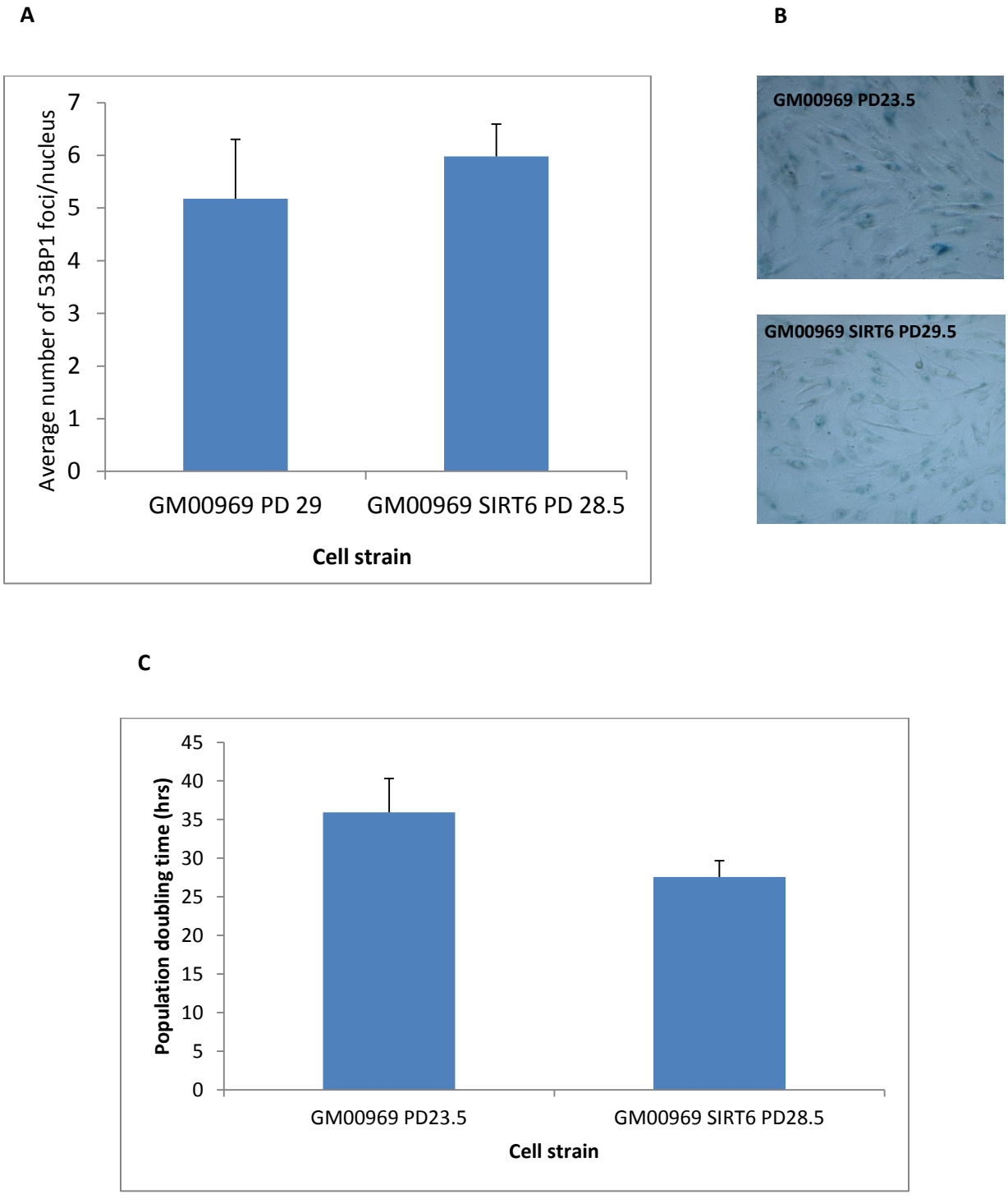

Figure 14. The Effects of SIRT6 Overexpression on GM00969 Normal Fibroblasts. *(A)* Average number of 53BP1-positive foci per nucleus. Data were derived from scoring 100 nuclei per sample. Error bars represent standard error (SE) (p-value=0.58). *(B)* Senescence-associated β-

gal staining in GM00969 fibroblasts ±SIRT6 overexpression. $1.5x10^4$ cells were seeded in triplicates in a 48-well dish and stained with β-gal staining solution 24 hours after plating. Images were captured at 20X magnification. *(C)* Proliferation rates of GM00969 fibroblasts ± SIRT6 overexpression. Bars represent the doubling time (hours) of each cell strain. Replicate values for doubling time were compared to GM00969 PD29. (p-value=0.16). Statistically significant results have a p value less than 0.05 (*p<0.05).

3.4 The Enzymatic Activity of SIRT6 as a Histone 3 Lysine 9 Deacetylase.

In order to determine the mechanism of action by which SIRT6 is exerting its biological function, the levels of acetylated H3K9 were examined in normal GM00969 fibroblasts and AG11513 fibroblasts ± SIRT6 overexpression via western blot (Figure 15). There seems to be a slight reduction in the levels of acetylated H3K9 in AG11513+SIRT6 fibroblasts, however there was no marked difference in the levels of acetylated H3K9 before and after ectopic SIRT6 expression.

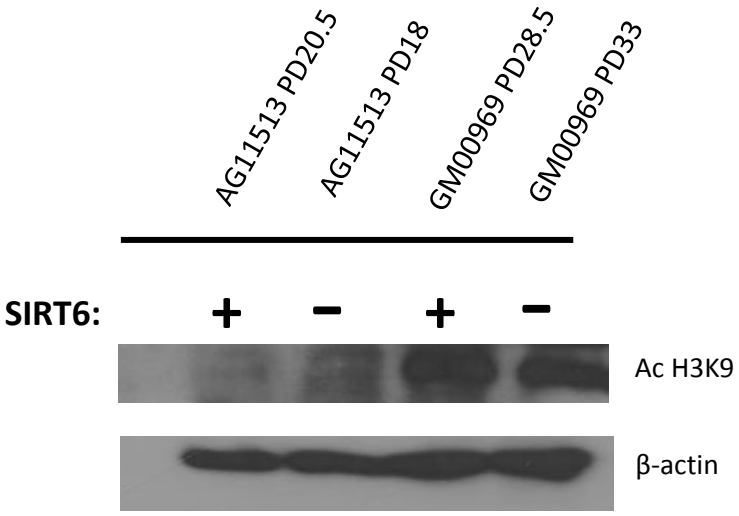

Figure 15. Western Blot to Assess Levels of Acetylated H3K9. HGPS (AG11513 PD18 and AG11513 SIRT6 PD20.5) and normal (GM00969 PD33 and GM00969 SIRT6 PD28.5) fibroblasts were assessed for the levels of acetylated H3K9 they expressed ± SIRT6 overexpression. There was no obvious reduction in the levels of acetylated H2K9.

To summarize findings from aim 2 of this study, SIRT6 was successfully and stably overexpressed in HGPS and normal fibroblasts. Immunofluorescence analysis confirmed that the overexpression was nuclear in cellular localization. In HGPS fibroblasts, SIRT6 overexpression resulted in a significant reduction (p-value= 0.01) in the frequency of 53BP1 foci per nucleus indicating a marked reduction in DNA damage in these cells. Also, the flattened senescent morphology previously seen in young PD HGPS fibroblasts was not observed in HGPS fibroblasts overexpressing SIRT6. Rather, these fibroblasts exhibited a spindle-like cellular morphology typical of healthy-looking fibroblasts derived from young donors. The proliferative capacity of HGPS fibroblasts overexpressing SIRT6 was also remarkably improved, with significantly shortened population doubling times when compared to parental uninfected HGPS fibroblasts (p-value=0.04). The same biological end-points were examined in normal fibroblasts ± SIRT6, showing slightly reduced β-gal positive staining and a shorter doubling time in normal fibroblasts overexpressing SIRT6 (not statistically significant).

4. DISCUSSION

HGPS is a childhood accelerated aging disease caused by a spontaneous point mutation in the *LMNA* gene. Progerin accumulates on the inner nuclear membrane, causing abnormalities in nuclear structure and function such as transcription, DNA replication, DNA repair, and the regulation of euchromatin-heterochromatin transitions. The nuclear architecture dysfunction not only leads to an accumulation of DNA damage in HGPS cells, but has also been proposed to be a contributing factor to telomere structure and function impairment. As a result of an impairment in DNA repair, DNA damage, namely in the form of DSBs, activates the DNA Damage Response pathway, which ultimately leads to cell cycle arrest and senescence. Cellular senescence has been reported as one of the major hallmarks of the aging process. As previously described, there are a number of cellular defects which lead to senescence such as telomere dysfunction and perturbations in chromatin organization. Changes in DNA methylation patterns, histone modifications and chromatin remodeling all constitute epigenetic modifications that also play a role in the pathological aspects of aging. Specific examples of alterations in heterochromatin factors in HGPS include decreased levels of heterochromatin protein (HP1), H3K9me3, and H3K27me3 and increased levels of H4K20me3. A recent study by Shah et al.[67] reported that lamin B1 levels decline during senescence and a forced lamin B1

reduction leads to premature senescence, concomitantly resulting in altered chromatin structure and reorganization in the human epigenome such as H3K4me3-enriched domains, which have also been detected in prematurely senescent HGPS cells. The results from this study indicated an indirect link between the formation of H3K4me3-enriched domains and accelerated tissue and organismal aging, possibly due to premature senescence chromatin changes.

SIRT6, a NAD^+-dependent protein deacetylase and ADP ribosyltransferase, has been studied extensively as a potential anti-aging factor. SIRT6 represents an epigenetically significant enzyme whose loss of function results in a progeroid phenotype in mice and whose gain of function extends longevity in mice, linking premature aging to altered chromatin at telomeres.

Despite the common degenerative phenotypes seen in SIRT6-deficient mice and HGPS, neither SIRT6 expression levels nor the manipulation of SIRT6 have been studied in HGPS fibroblasts. **Thus, the first goal of this study was to determine whether HGPS fibroblasts express lower levels of SIRT6 than normal fibroblasts. Moreover, cellular features such as persistent DNA damage, β-galactosidase positivity and reduced proliferative capacity, which collectively suggest cellular senescence, were assessed in HGPS fibroblasts relative to normal fibroblasts of young and old donor age in order to generate baseline data for the overexpression studies in Aim 2.**

Here we show that SIRT6 protein levels were markedly reduced in all 3 typical HGPS strains compared to normal fibroblasts. Unlike typical HGPS strains, atypical HGPS cells do not express

progerin and were found to express higher SIRT6 levels than typical HGPS cells. The fact that only progerin expressing cells expressed low endogenous levels of SIRT6 raised a question, whether a relationship exists between progerin production and SIRT6 expression. The level of SIRT6 protein expression was also assessed in 3 independent immunofluorescence (IF) assays showing a consistent reduction in signal intensity in typical HGPS fibroblasts compared to normal fibroblast controls. qRT-PCR was conducted to explore whether SIRT6 was reduced at the transcriptional level. Preliminary results showed a significant reduction in the mRNA levels of SIRT6 in typical HGPS cells relative to normal fibroblasts, which suggests that SIRT6 expression may be at least in part regulated at the transcriptional level. However, mRNA assessment must be repeated in order to ensure validity of results and reproducibility. Nonetheless, the consistency of protein results with typical HGPS cell strains derived from 3 different donors obtained from western analysis coupled with the IF assays allows for a confident conclusion that typical HGPS fibroblasts express lower levels of SIRT6 than normal fibroblasts.

Three different markers of cellular senescence were examined in typical HGPS fibroblasts and compared to normal fibroblasts of comparable population doublings. The first endpoint examined was DNA damage in the form of DNA double-strand breaks. The frequency of 53BP1 foci in typical HGPS fibroblasts (AG11513, 8 year old donor) was examined by IF and compared to normal strains from 2 year old (GM00969) and 92 year old (AG09602) donors. Results revealed that AG11513 cells at PD11.5 had an average frequency of 5.9 foci per nucleus while GM00969 PD29 had 5.2 foci per nucleus. These PDs were considered relatively young for both samples. In similar culture conditions, HGPS fibroblasts were seen to have a maximum

replicative capacity at PD30-35, while GM00969 fibroblasts grew exponentially until PD40-50. Although there was no statistical significance (p-value= 0.7) between the average number of 53BP1 DNA damage foci in HGPS vs. normal fibroblasts, the closeness in the frequency of foci considering the 18 population doubling gap is consistent with early onset of DNA damage in the HGPS fibroblasts. Furthermore, although not significant, a trend towards an increase in foci frequency with increasing replicative age was observed in AG11513 PD11.5 versus PD24, but not in GM00969 PD29 versus PD41. This is suggestive that in culture, an accumulation of DNA damage can be seen in HGPS fibroblasts with time, while the number of 53BP1 foci in normal fibroblasts remains seemingly constant. It is necessary, however, to observe the frequency of 53BP1-positive foci in AG11513 fibroblasts at a closer PD to the normal fibroblasts to which we are comparing. We predict a significantly higher frequency of 53BP1 DNA-damage foci in HGPS fibroblasts than in normal fibroblasts of the same PD. Finally, AG09602 normal fibroblasts at PD17 showed a significantly high frequency of 53BP1 foci (15 foci per nucleus) which is consistent with reports that DNA damage accumulates with older physiological age.[62]

The second biological end point examined as a biomarker for cellular senescence was SA β-gal activity. This assay was used to determine the frequency of senescence in HGPS fibroblasts compared to normal fibroblasts from young (GM00969) and old (AG09602) donors. The frequency of β-gal positive cells could not be quantitatively determined due to a non-specific blue hue that renders it difficult to differentiate a β-gal positive cell from a non-specifically stained cell. As a result, classifying cells as being positively or negatively stained would be a subjective matter and irreproducible. Also, in cells that are in fact positively stained, it is difficult to quantify the intensity of blue staining and cells with strong, moderate or weak blue

staining would all be considered equally positive. An additional limitation of using this assay is that under the microscope, different fields of the same sample may have different staining intensities depending on the confluency of cells. SA β-gal staining has been found to be more intense in areas where cells are more confluent. Therefore, it is important to ensure that the distribution of cells in replicate wells is uniform and multiple fields are scored. Despite these limitations, the SA β-gal assay was chosen to assess cellular senescence due to its simplicity and robust detection of β-gal activity in cells exhibiting an enlarged and flattened senescent morphology. By means of visual inspection, young AG11513 fibroblasts (PD20.5) exhibited staining intensities comparable to GM00969 fibroblasts almost 23 PDs higher. Also, while low passage GM00969 and AG09602 fibroblasts displayed the typical fusiform morphology of healthy fibroblasts, AG11513 fibroblasts as early as PD10.5 displayed an enlarged, flattened cellular morphology consistent with a senescent state. Findings from the SA β-gal studies showed that normal and HGPS fibroblasts displayed more intense staining with increasing time with culture and HGPS fibroblasts exhibited senescent cellular phenotypes at remarkably low passage numbers suggestive of premature replicative senescence. Here, we used SA β-gal as a qualitative assessment of cellular senescence; however, alternative methods can be employed in order to generate future quantitative data. An assay developed by Shiush et al.[58] employs the SA β-gal staining technique followed by the capture and digital analysis of the stained cells. They have reported that this method of quantifying SA β-gal activity is accurate and reproducible in detecting cellular senescence. Markers of cellular senescence such as the cell-cycle inhibitors p16 and p21 may also be looked at as an alternative method of identifying senescent cells.

There is persistent activation of the ATM/ATR pathway in HGPS cells due in part, to the accumulation of DNA damage. As a result, there is a reduction in cell cycle progression and replicative capacity which contribute to pathological aging.[29,33] The doubling times of HGPS and normal fibroblasts was the third biological end point assessed in order to investigate their replicative state. As anticipated, fibroblasts from 2 different HGPS donors had significantly longer doubling times than normal fibroblasts of comparable population doublings. Also in normal and HGPS fibroblasts, a trend towards longer doubling times with increasing replicative age was observed. The interpretation of this data suggests that HGPS fibroblasts have a lower proliferation capacity than normal fibroblasts, which progressively lessens with replicative age.

Data generated from the first part of this study revealed for the first time that HGPS fibroblasts express lower levels of SIRT6 protein and mRNA than normal fibroblasts. This comparative analysis also demonstrated that HGPS fibroblasts exhibit more DNA damage, more pronounced β-gal staining coupled with a senescent cellular morphology, and a longer population doubling time than normal fibroblasts at an equal or higher PD, as previously reported.[63] This begs the question: Will SIRT6 overexpression in HGPS fibroblasts prevent (or possibly reverse) this accelerated aging phenotype? The second part of this study encompassed a series of *in vitro* experiments to begin to answer this question.

We first stably overexpressed SIRT6 in HGPS and normal fibroblasts using a lentiviral vector. In order to ensure the biological end points assessed were solely due to the effects of the SIRT6 gene, an empty lentivector control was included. However, contrary to the SIRT6 infected cells, after a couple of population doublings, the empty vector control cells were no longer viable,

providing an initial indication that SIRT6 was exerting a growth advantage to the HGPS fibroblasts. Then, paralleling the senescence characterization in Aim 1, we assessed the frequency of 53 BP1 DNA damage foci, β-gal histochemical staining and proliferative capacity in SIRT6-infected HGPS fibroblasts compared to parental controls. We conjectured that sustained SIRT6 expression may prevent or at least minimize the DNA damage and the development of senescence-like features in HGPS cells.

Here we indeed demonstrate that overexpression of SIRT6 in HGPS fibroblasts resulted in a marked reduction in the frequency of 53BP1 foci when compared to uninfected HGPS control fibroblasts. This significant reduction in the average number 53BP1 positive foci per nucleus correlates with a fewer incidence of DSBs and ultimately a reduction in DNA damage.

Moreover, SA β-gal staining was examined ± SIRT6 infection in HGPS fibroblasts. As earlier mentioned, low passage HGPS cells exhibited extensive staining as well as an irregular, senescent cellular morphology. Visibly, there was no reduction in intensity of β-gal staining after SIRT6 overexpression, which may be attributable to possible nonspecific staining (i.e. all cells were stained blue to some degree). However, the classic senescent morphology previously seen in the HGPS fibroblasts as early as PD10.5 was not observed in the SIRT6 infected HGPS fibroblasts even at PD20.5. It seems that ectopically expressing SIRT6 is either delaying the onset of senescence to some extent or possibly mitigating the senescent cellular morphology. Again, more quantitative approaches need to be employed before making a compelling conclusion.

Finally, the effect of SIRT6 overexpression on the proliferative capacity of HGPS fibroblasts was examined. A significant reduction in the doubling times of SIRT6 infected HGPS fibroblasts was observed compared to parental uninfected controls at both young and older population doublings. Although statistically insignificant, the doubling time of uninfected HGPS fibroblasts doubled as they aged in culture from PD12.5 to PD20. Whereas, there was almost no change in the doubling time of SIRT6 infected HGPS fibroblasts from PD12 to PD18.5. It can be concluded from these findings that SIRT6 overexpression led to an improvement in proliferative capacity in HGPS fibroblasts.

To further examine whether SIRT6 overexpression offers a growth advantage to normal fibroblasts as well as HGPS fibroblasts, the effects of SIRT6 overexpression were assessed in normal GM00969 fibroblasts. There was no significant difference in the frequency of 53BP1 DNA damage foci in normal fibroblasts overexpressing SIRT6 compared to uninfected normal fibroblasts. Additionally, although slightly less intense in GM00969+SIRT6, β-galactosidase staining was equally minimal in GM00969 with (PD29.5) or without (PD23.5) ectopic SIRT6 expression. We observed shorter population doubling times in GM00969 SIRT6 PD28.5 fibroblasts when compared to GM00969 PD23.5; however, these results were also statistically insignificant. Overall, preliminary results indicated that SIRT6 overexpression did not have pronounced beneficial effects on normal fibroblasts as it did on HGPS fibroblasts. However, we have established that normal fibroblasts express substantial SIRT6 protein levels, the overexpression of which seems to offer no additional benefit in terms of the reduction of DNA damage and prevention of senescence. Assessing these end points after aging the normal fibroblasts longer in culture to when they typically present a more pronounced senescent

phenotype could provide more insight into effect of SIRT6 on preventing the onset of senescence. Also, using siRNA to silence SIRT6 expression in normal fibroblasts and evaluating the effects of minimal/no SIRT6 protein in normal fibroblasts could be a plausible experiment to conduct. It would be of great interest to examine whether re-introducing SIRT6 in the SIRT6 knock down normal fibroblasts results in a rescue of the senescent phenotype.

In summary, the goal of this study was to determine whether HGPS fibroblasts exhibited lower levels of SIRT6 than normal fibroblasts and whether reduced SIRT6 expression contributes to the premature senescence phenotype of HGPS fibroblasts. Cellular senescence is one of the major hallmarks of aging, and this study aimed to delve into several of the cellular defects leading to cellular senescence and how they may be prevented. Epigenetic changes such as altering histone methylation have been found to induce lifespan extension in nematodes and flies.[58,59] For this reason, along with previous studies assessing the role of SIRT6 on genomic stability and longevity,[41,45] it is reasonable to examine the effects of manipulating a histone-modifying enzyme such as SIRT6 on the various aspects of aging in HGPS. This study revealed that typical HGPS fibroblasts express lower levels of SIRT6 protein and mRNA than atypical HGPS fibroblasts and normal fibroblasts derived from young and old donors. The expression of progerin protein is what sets apart typical HGPS fibroblasts from atypical HGPS and normal fibroblasts. For this reason, it can be proposed that there may be a link between progerin expression and SIRT6 expression levels. However, when progerin expression was induced in normal HDFs to levels similar to those of HGPS fibroblasts, no effect on the expression of SIRT6 protein was observed. Thus, it is possible that progerin is not directly interfering with SIRT6

expression in HGPS cells and there may be other mechanisms unique to HGPS, by which these cells express relatively lower levels of SIRT6.

The presence of DNA damage, β-galactosidase positivity, and low proliferative capacity were anticipated in HGPS fibroblasts and all agreed with previous reports.[14,29] However, do these cellular defects correlate with the low levels of SIRT6 expressed in HGPS fibroblasts? The results of the experiments conducted following SIRT6 overexpression showed a significant reduction in DNA damage and improvement in proliferative capacity. β-gal activity did not appear to be affected by SIRT6 overexpression and remains to be quantitatively measured; however, the SIRT6 infected HGPS fibroblasts exhibited a healthier cellular phenotype, which could be indicative of a mild improvement of the pronounced senescent phenotype of HGPS fibroblasts. Taken together, these findings indicate that low SIRT6 expression levels in HGPS fibroblasts positively correlates with premature senescence, which can be prevented by overexpressing SIRT6. This is further indication that epigenetic changes may be a contributing factor to the aging process and manipulation of the histone deacetylase SIRT6 may improve several aspects of aging. It is necessary, however, to identify the mechanism by which SIRT6 is modulating senescence. To begin to elucidate mechanism, we attempted to demonstrate that SIRT6 overexpressing fibroblasts exhibit an overall reduction in the level of acetylated H3K9, as would be expected for cells ectopically expressing functional SIRT6. However, western blot analysis revealed no reduction in acetylated H3K9 levels in HGPS and normal fibroblasts overexpressing SIRT6 compared to uninfected parental controls. A possible reason for this could be that SIRT6 has poor H3K9 deacetylase activity *in vitro*. Gil et al.[60] revealed that SIRT6 showed significant deacetylase activity when histones were packaged as nucleosomes, as opposed to using

unpackaged histones. Therefore, determining SIRT6 functionality is a critical limitation of the data set and must be further explored before conclusions can be made on the mechanism of action of the SIRT6 enzyme.

Assuming the characterized H3K9 deacetylase activity of SIRT6[49], hyperacetylation due to SIRT6 deficiency is thought to interfere with the association of DNA repair proteins at the telomeres suggesting that an altered chromatin state may be required for the recruitment of telomere binding proteins.[62] It would be helpful to assess the recruitment of DNA repair proteins such as DNA-PKs to DSBs following SIRT6 overexpression to further elucidate mechanistic details concerning the functional role of SIRT6 in the context of DNA repair and genomic stability. Furthermore, a hyperacetylated chromatin state, particularly at the telomeres, is associated with an opened chromatin structure which leads to the replication and metabolism of telomeres. Ectopically expressing SIRT6 may lead to a reduction in acetylated H3K9 levels and consequently a condensed chromatin structure and transcriptional silencing. This may prove very beneficial in HGPS since they originally have short telomeres and silencing their transcription may prevent the progressive telomere shortening which occurs during replication. In this regard, SIRT6 expression in HGPS fibroblasts may play a role in preventing DNA damage-induced and telomere-induced senescence (Figure 16).

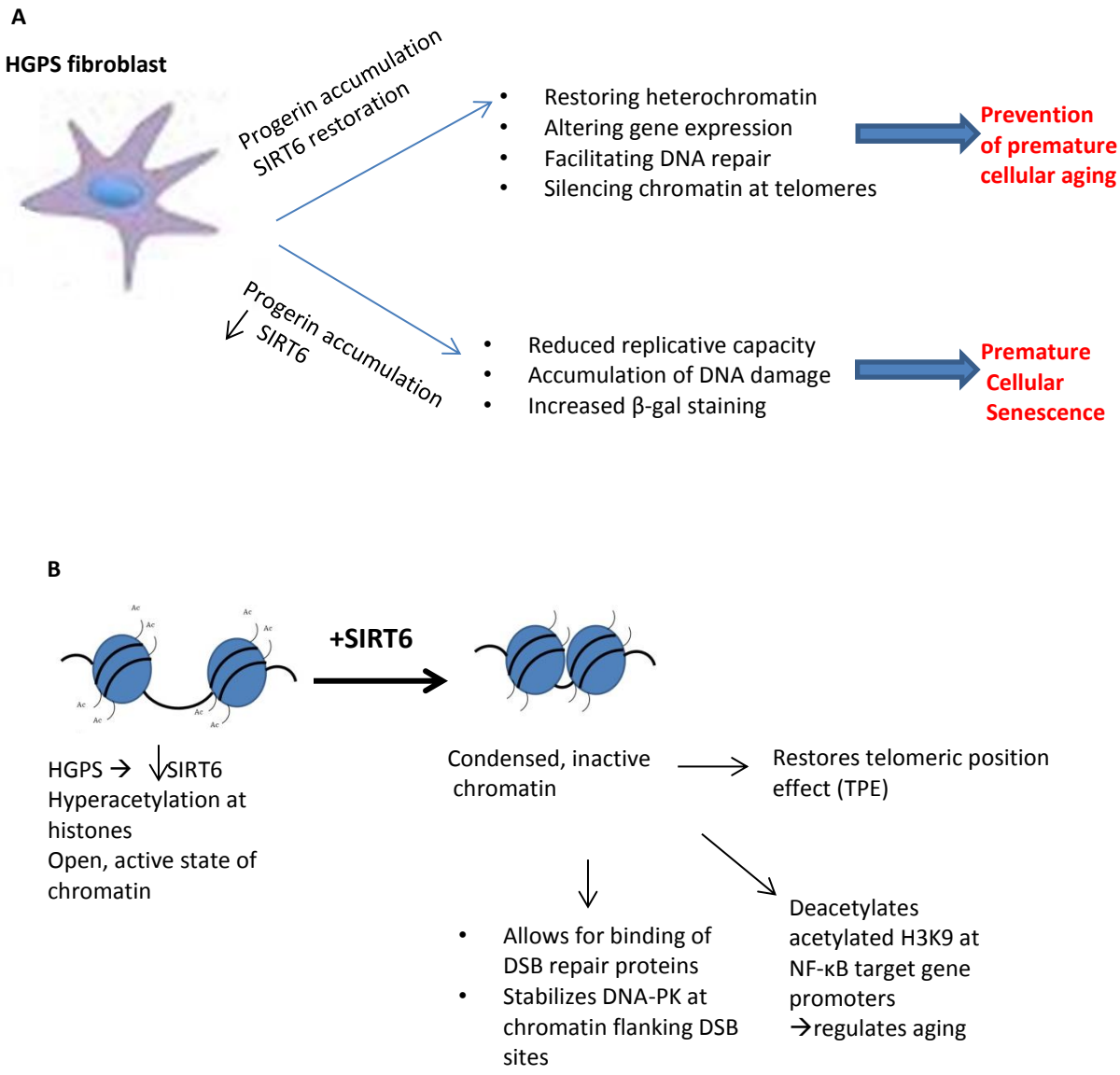

Figure 16. A proposed schematic summarizing the effects of SIRT6 on HGPS cells.

This study has shown important implications of manipulating SIRT6 to counteract the premature cellular senescence in HGPS and ultimately prevent the accelerated aging phenotype. Studies have shown that SIRT6 deficiency produces premature aging phenotypes coinciding with those observed in HGPS, while overexpressing SIRT6 promotes longevity in male mice.[39,41-45] In this context, our findings that HGPS fibroblasts express low levels of SIRT6 and that overexpressing SIRT6 positively correlates with an attenuation of the cellular defects contributing to premature senescence suggest that increasing the levels of this protein may be a viable approach to delay aging in HGPS. It is necessary however, to assess the end points examined over a longer duration to determine whether SIRT6 overexpression helps to elongate the lifespan of HGPS cells. Due to the common involvement of progerin in both HGPS and normal aging, it will be of great interest to see if the mechanism of action of SIRT6 is also true in normal aging.[30]

List of References

List of References

1 Serio, R. N. (May 19 2011). Unraveling the Mysteries of Aging Through a Hutchinson Gilford Progeria Syndrome Model. Rejuvenation Research, 14(2), 133-141

2 D'Apice, R. M., Tenconi, R., Mammi, I., van den Ende, J., & Novelli, G. (2004). Paternal origin of LMNA mutations in Hutchinson–Gilford progeria.*Clinical Genetics*, *65*(1), 52-54

3 Jean-Ha Baek, Tomás McKenna and Maria Eriksson (2013). Hutchinson-Gilford Progeria Syndrome, Genetic Disorders, Prof. Maria Puiu (Ed.), ISBN: 978-953-51-0886-3, InTech, DOI: 10.5772/53794. Available from: http://www.intechopen.com/books/genetic-disorders/hutchinson-gilford-progeria-syndrome

4 Kieran, M., Gordon, L., & Kleinman, M. (2007). New approaches to progeria. *Pediatrics*, *120*(4), 834-884.

5 Eriksson M, Brown WT, Gordon LB, Glynn MW, Singer J, Scott L, Erdos MR, Robbins CM, Moses TY, Berglund P, Dutra A, Pak E, Durkin S, Csoka AB, Boehnke M, Glover TW and Collins FS. (2003). Recurrent de novo point mutations in lamin A cause Hutchinson-Gilford progeria syndrome. *Nature*, *423*(6937), 293-298.

6 Garg A, Subramanyam L, Agarwal AK, Simha V, Levine B, D'Apice MR, Novelli G, Crow Y. (2009). Atypical Progeroid Syndrome due to Heterozygous Missense *LMNA* Mutations. *J Clin Endocrinal Metab.*, 94(12), 4971-4983.

7 Liang L, Zhang H, Gu X. (2009). Homozygous LMNA mutation R527C in atypical Hutchinson–Gilford progeria syndrome: Evidence for autosomal recessive inheritance. *Acta paediatr,* 98(8), 1365-1368.

8 Beck, L. A., Hosick, T. J. & Sinensky, M. (1990) Isoprenylation is required for the processing of the lamin A precursor. *J. Cell Biol.* 110, 1489–1499.

9 Capell, B. C., & Collins, F. S. (2006). Human laminopathies: Nuclei gone genetically awry. *Nature Revies Genetics*, *7*, 950-952.

10 Goldman RD, et al. (2004) Accumulation of mutant lamin A causes progressive changes in nuclear architecture in Hutchinson-Gilford progeria syndrome. *Proc Natl Acad Sci U S A*, 101(24), 8963–8968.

11 López-Otín, C., Blasco, M. A., Partridge, L., Serrano, M., & Kroemer, G. (2013). The Hallmarks of Aging. *Cell*,*153*(6), 1194-1217.

12 Decker, M. L., Chavez, E., Vulto, I., & Lansdorp, P. M. (2009). Telomere length in Hutchinson-Gilford progeria syndrome. *Mechanisms of Ageing and Development*, *130*, 377-383.

13 Aubert, G., & Lansdorp, P. M. (2008). Telomeres and aging. *Physiol Rev*, *88*, 577-579.

14 Cao, K., Blair, C. D., Faddah, D. A., Kieckhaefer, J. E., Olive, M., Erdos, M. R., Nabel, E. G., & Collins, F. S. (2011). Progerin and telomere dysfunction collaborate to trigger cellular senescence in normal human fibroblasts. *J Clin Invest.*, *121*(7), 2833-2844.

15 Henson JD, Neumann AA, Yeager TR, Reddel RR (2002). Alternative lengthening of telomeres in mammalian cells" Oncogene 21(4) 598-610.

16 Andrey Grach (2013). Telomere Shortening Mechanisms, The Mechanisms of DNA Replication, Dr. David Stuart (Ed.), ISBN: 978-953-51-0991-4, InTech, DOI: 10.5772/55244. Available from: http://www.intechopen.com/books/the-mechanisms-of-dna-replication/telomere-shortening-mechanisms

17 Ji, G., Liu, K., Okuka, M., Liu, N., & Liu, L. (2012). Association of telomere instability with senescence of porcine cells. *BMC Cell Biology*, *13*(36).

18 Campisi, J. (1997). The biology of replicative senescence .*Eur J Cancer*, *33*(5), 703-709.

19 van Steensel, B., Smogorzewska, A., & de Lange , T. (1998). Trf2 protects human telomeres from end-to-end fusions. *Cell*, *92*(3), 401-413.

20 Campisi J. Senescent cells, tumor suppression, and organismal aging: Good citizens, bad neighbors. Cell 2005;120:513–522.

21 Lombard , D. B., Chua, K. F., Mostoslavsky, R., Franco, S., Gostissa , M., & Alt, F. W. (2005). DNA repair, genome stability, and aging . *Cell*, *120*, 497-512.

22 Bodnar A.G., Ouellette M., Frolkis M., Holt S.E., Chiu C.P., Morin G.B., Harley C.B., Shay J.W., Lichtsteiner S., Wright W.E. (1998). Extension of life-span by introduction of telomerase into normal human cells. *Science*, 279(5349), 349-352.

23 Vaziri, H., & Benchimol, S. (1998). Reconstitution of telomerase activity in normal human cells leads to elongation of telomeres and extended replicative life span. *Cell*, *8*(5), 279-282.

24 Oullette, M. M., McDaniel, L. D., Wright, W. E., Shay, J. W., & Schultz , R. A. (2000). The establishment of telomerase-immortalized cell lines representing human chromosome instability syndromes. *Hum. Mol. Genet.*, *9*(3), 403-411.

25 Allsopp, R.C., Vaziri, H., Patterson, C., Goldstein, S., Younghai, E.V., Futcher, A.b., Greider, C.W., & Harley, C.B. (1992) Telomere length predicts replicative capacity of human fibroblasts. *Proc. Natl Acad. Sci. USA,* 89, 10114-10118.

26 Dimri GP, Lee X, Basile G, Acosta M, Scott G, Roskelley C, Medrano EE, Linskens M, Rubelj I, Pereira-Smith O, et al. (1995). A biomarker that identifies senescent human cells in culture and in aging skin in vivo. *Cell biology,* 92, 9363-9367.

27 Gordon et. al. (2012). Clinical Trial of a Farnesyltransferase Inhibitor in Children with Hutchinson-Gilford Progeria Syndrome, *PNAS*, 109(41), 16666-16671

28 Yang, S. H., Qiao, X., Fong, L. G. & Young, S. G (2008).Treatment with a farnesyltransferase inhibitor improves survival in mice with a Hutchinson-Gilford progeria syndrome mutation. *Biochim. Biophys. Acta* 1781(1-2), 36–39.

29 Musich PR, Zou Y (2011). DNA-damage accumulation and replicative arrest in Hutchinson-Gilford progeria syndrome. *Biochem Soc Trans*, 39, 1764-1769

30 McClintock D, Ratner D, Lokuge M, Owens DM, Gordon LB, et al. (2007) The Mutant Form of Lamin A that Causes Hutchinson-Gilford Progeria Is a Biomarker of Cellular Aging in Human Skin. *PLoS ONE,* 2(12), e1269

31 Musich PR, Zou Y (2009). Genomic instability and DNA damage responses in progeria arising from defective maturation of prelamin A. *Aging,* 1(1), 28-37

32 d'Adda di Fagagna F, Reaper PM, Clay-Farrace L, Fiegler H, Carr P, Von Zglinicki T, Saretzki G, Carter NP, Jackson SP (2003). A DNA damage checkpoint response in telomere-initiated senescence. *Nature,* 426, 194-198

33 Liu, Y., Rusinol, A., Sinensky, M., Wang, Y. & Zou, Y. (2006). DNA damage responses in progeroid syndromes arise from defective maturation of prelamin A. *Journal of Cell Science*, 119, 4644-4649

34 Benson, E. K., Lee, S. W., & Aaronson, S. A. (2010). Role of progerin-induced telomere dysfunction in HGPS premature cellular senescence. *Journal of Cell Science*, *123*, 2605-2612.

35 Anderson, L., Henderson, C., & Adachi, Y. (2001). Phosphorylation and rapid relocalization of 53BP1 to nuclear foci upon DNA damage. *Molecular and Cellular Biology*, *21*(5), 1719-1729.

36 Fitzgerald , J. E., Grenon, M., & Lowndes, N. F. (2009). 53BBP1: Function and mechanisms of focal recruitment. *Biochem. Soc. Trans*, *37*, 897-904.

37 Dekker, P., de Lange, M.J., Dirks, R.W., van Heemst, D., Tanke, H.J., Westendorp, R.G., Maier, A.B. (2011). Relation Between Maximum Replicative Capacity and Oxidative Stress-Induced Responses in Human Skin Fibroblasts In Vitro. *J Gerontol A Biol Sci Med Sci.,* 66A(1), 45–50.

38 Liu, B., Wang, J., Chan, K.M., Tjia, W.M., Deng, W., Guan, X., Huang, J.D., Li, K.M., Chau, P.Y., Chen, D.J., Pei, D., Pendas, A.M., Cadiñanos, J., López-Otín, C., Tse, H.F., Hutchison, C., Chen, J., Cao, Y., Cheah, K.S., Tryggvason, K., Zhou, Z. (2005). Genomic instability in laminopathy-based premature aging. *Nature medicine*, 11(7), 780-785

39 Jia, G., Su, L., Singhal, S., & Liu, X. (2012). Emerging roles of SIRT6 on telomere maintenance, DNA repair, metabolism and mammalian aging. *Mol Cell Biochem*, 364, 345-350.

40 McCord, R.A., Michishita, E., Hong, T., Berber, E., Boxer, L.D., Kusumoto, R., Guan, S., Shi, X., Gozani, O., Burlingame, A.L., Bohr, V.A., & Chua, K.F. (2009). SIRT6 stabilizes DNA-dependent protein kinase at chromatin for DNA double-strand break repair. *Aging,* 1(1), 109-121,

41 Kanfi Y, Naiman S, Amir G, Peshti V, Zinman G, Nahum L, Bar-Joseph Z, Cohen HY. (2012). The sirtuin SIRT6 regulates lifespan in male mice. *Nature,* 483, 218-221.

42 Mostoslavsky R, Chua KF, Lombard DB, Pang WW, Fischer MR, Gellon L, Liu P, Mostoslavsky G, Franco S, Murphy MM, Mills KD, Patel P, Hsu JT, Hong AL, Ford E, Cheng HL, Kennedy C, Nunez N, Bronson R, Frendewey D, Auerbach W, Valenzuela D, Karow M, Hottiger MO, Hursting S, Barrett JC, Guarente L, Mulligan R,Demple B, Yancopoulos GD, Alt FW. (2006). Genomic Instability and Aging-like Phenotype in the Absence of Mammalian SIRT6. *Cell*, 124, 315-329.

43 Tennen RI, Chua KF. (2011). Chromatin regulation and genome maintenance by mammalian SIRT6. *Trends Biochem Sci., 36(1),* 39-46.

44 Cardus A, Uryga AK, Walters G, Erusalimsky JD. (2013). SIRT6 protects human endothelial cells from DNA damage, telomere dysfunction, and senescence. *Cardiovascular Research*, 97, 571-579.

45 Kaeberlein M, McVey M, Guarente L. (1999). The *SIR2/3/4* complex and *SIR2* alone promote longevity in *Saccharomyces cerevisiae* by two different mechanisms. *Genes Dev.,* 13(19), 2570-2580.

46 M. Kaeberlein, C. Burtner, B. Kennedy (2007). "Recent Developments in Yeast Aging". *PLOS Genetics,* 3 (5), 655–660.

47 Rottem, S., & Barile, M.F. (1993). Beware of mycoplasmas. *Cell*, 11(4), 143-151.

49 Michishita E, McCord RA, Berber E, Kioi M, Padilla-Nash H, Damian M, Cheung P, Kusumoto R, Kawahara TL, Barrett JC, Chang HY, Bohr VA, Ried T, Gozani O,Chua KF. (2008). SIRT6 is a histone H3 lysine 9 deacetylase that modulates telomeric chromatin, *Nature,* 452(7186), 492–496.

50 Ross WE, Bradly MO. (1981). DNA double-strand breaks in mammalian cells after exposure to intercalating agents. *BBA,* 654, 129-134

51 Elmore LW, Rehder CW, Di X, McChesney PA, Jackson-Cook CK, Gewirtz DA, Holt SE. (2002). Adriamycin-induced Senescence in Breast Tumor Cells Involves Functional p53 and Telomere Dysfunction. *J Biol Chem, 227(38)*

52 Bradford, M.M. (1976). A dye binding assay for protein. *Anal. Biochem*., 72, 248-254

53 SuperSignal West Pico Chemiluminescent substrate, Thermo Scientific. http://www.piercenet.com/browse.cfm?fldID=01041101

54 Thellin O, Zorzi W, Lakaye B, De Borman B, Coumans B, Hennen G, Grisar T, Igout A, Heinen E. (1999). Housekeeping genes as internal standards: use and limits. *J biotechnol,* 75(2-3), 291-295

55 Livak, K.J., & Schmittgen, T.D. (2001). Analysis of Relative Gene Expression Data Using Real-Time Quantitative PCR and the $2^{-\Delta\Delta C}{}_{T}$ Method. *Methods*, 25, 402-208.

56 Sedelnikova, O.A., Horikawa, I., Zimonjic, D.B., Popescu, N.C., Bonner W.M., Barrett, J.C. (2004). Senescing human cells and ageing mice accumulate DNA lesions with unrepairable double-strand breaks. *Nature Cell Biology*, 6, 168-170.

57 Shiush, L.I., Itzkovitz, S., Cohen, A., Rutenberg, A., Berkovitz, R., Yehezkel, S., Shahar, H., Selig, S., & Skorecki, K. (2011). Quantitative digital *in situ* senescence-associated β-galactosidase assay. *BMC Cell Biology*, 12(16).

58 Greer, E.L., Maures, T.J., Hauswirth, A.G., Green, E.M., Leeman, D.S., Maro, G.S., Han, S., Banko, M.R. Gozani, O., and Brunet, A. (2010). Members of the H3K4 trimethylation complex regulate lifespan in a germline-dependent manner in C.elegans. *Nature,* 466,383-387.

59 Siebold, A.P., Banerjee, R., Tie, F., Kiss, D.L., Moskowitz, J., and Harte, P.J. (2010). Polycomb Repressive Complex 2 and Trithorax modulate Drosophila longevity and stress resistance. *Proc. Natl. Acad. Sci. USA,* 107, 169-174.

60 Gil R, Barth S, Kanfi Y, Cohen HY (2013) SIRT6 exhibits nucleosome-dependent deacetylase activity. *Nucleic Acid Res.*, 41(18), 8537-8545.

61 Tennen RI, Bua DJ, Wright WE, Chua KF. (2011). SIRT6 is required for maintenance of telomere position effect in human cells. *Nat. Commun*. 2 (433).

62 Burtner, C.R., Kennedy, B.K. (2010). Progeria syndromes and ageing: What is the connection? *Nature Reviews,* 11, 567-578.

63 Goldman, R. D., Gruenbaum, Y., Moir, R. D., Shumaker, D. K., & Spann, T. P. (2002). Nuclear lamins: building blocks of nuclear architecture. *Genes & development*, 16(5), 533-47

64 Gruenbaum, Y., Margalit, A., Goldman, R. D., Shumaker, D. K., & Wilson, K. L. (2005). The nuclear lamina comes of age. *Nature reviews Molecular cell biology.*, 6(1), 21-31

65 Boban, M., Braun, J., & Foisner, R. (2010). Lamins:'structure goes cycling'. *Biochemical Society transactions,* 38(1), 301-306

65 Liszt G, Ford E, Kurtev M, Guarente L. (2005). Mouse Sir2 homolog SIRT6 is a nuclear ADP-ribosyltransferase. *J Biol Chem*., 280, 21313–21320

67 Shah, P.P., Donahue, G., Otte, G.L., et al. (2013). Lamin B1 depletion in senescent cells triggers large-scale changes in gene expression and the chromatin landscape. *Genes Dev,* 27, 1787-1799.

Vita

Helal Abdurrazak Ali Endisha was born on August 12, 1989, in London, United Kingdom and is a British citizen. She graduated from International School of Choueifat, Cairo, Egypt in 2006. She graduated with honors from the German University in Cairo in 2011, where she received her Bachelor of Science in Pharmacy and Biotechnology.